

# Synthesis, properties, and biological activity of boranophosphate analogs of the mRNA cap: versatile tools for manipulation of therapeutically relevant cap-dependent processes

Joanna Kowalska<sup>1</sup>, Anna Wypijewska del Nogal<sup>1</sup>, Zbigniew M. Darzynkiewicz<sup>1</sup>, Janina Buck<sup>2</sup>, Corina Nicola<sup>2</sup>, Andreas N. Kuhn<sup>2,3</sup>, Maciej Lukaszewicz<sup>1</sup>, Joanna Zuberek<sup>1</sup>, Malwina Strenkowska<sup>1</sup>, Marcin Ziemniak<sup>1</sup>, Maciej Maciejczyk<sup>4</sup>, Elzbieta Bojarska<sup>5</sup>, Robert E. Rhoads<sup>6</sup>, Edward Darzynkiewicz<sup>1,5</sup>, Ugur Sahin<sup>2,3</sup> and Jacek Jemielity<sup>1,5,\*</sup>

<sup>1</sup>Division of Biophysics, Institute of Experimental Physics, Faculty of Physics, University of Warsaw, Warsaw, Poland, <sup>2</sup>BioNTech RNA Pharmaceuticals GmbH, Mainz, Germany, <sup>3</sup>TRON—Translational Oncology at the University Medical Center Mainz, Germany, <sup>4</sup>University of Warmia and Mazury in Olsztyn, Olsztyn, Poland, <sup>5</sup>Centre of New Technologies, University of Warsaw, Poland and <sup>6</sup>Department of Biochemistry and Molecular Biology, LSU Health Sciences Center, Shreveport, LA 71130, USA

Received May 19, 2014; Revised August 05, 2014; Accepted August 6, 2014

## ABSTRACT

Modified mRNA cap analogs aid in the study of mRNA-related processes and may enable creation of novel therapeutic interventions. We report the synthesis and properties of 11 dinucleotide cap analogs bearing a single boranophosphate modification at either the  $\alpha$ -,  $\beta$ - or  $\gamma$ -position of the 5',5'-triphosphate chain. The compounds can potentially serve either as inhibitors of translation in cancer cells or reagents for increasing expression of therapeutic proteins *in vivo* from exogenous mRNAs. The BH<sub>3</sub>-analogs were tested as substrates and binding partners for two major cytoplasmic cap-binding proteins, DcpS, a decapping pyrophosphatase, and eIF4E, a translation initiation factor. The susceptibility to DcpS was different between BH<sub>3</sub>-analogs and the corresponding analogs containing S instead of BH<sub>3</sub> (S-analogs). Depending on its placement, the boranophosphate group weakened the interaction with DcpS but stabilized the interaction with eIF4E. The first of the properties makes the BH<sub>3</sub>-analogs more stable and the second, more potent as inhibitors of protein biosynthesis. Protein expression in dendritic cells was 2.2- and 1.7-fold higher for mRNAs capped with m<sub>2</sub><sup>7,2'-O</sup>Gpp<sub>BH3</sub>pG D1 and m<sub>2</sub><sup>7,2'-O</sup>Gpp<sub>BH3</sub>pG D2, respectively, than for *in vitro* transcribed mRNA capped with m<sub>2</sub><sup>7,3'-O</sup>GpppG. Higher expression of

cancer antigens would make mRNAs containing m<sub>2</sub><sup>7,2'-O</sup>Gpp<sub>BH3</sub>pG D1 and m<sub>2</sub><sup>7,2'-O</sup>Gpp<sub>BH3</sub>pG D2 favorable for anticancer immunization.

## INTRODUCTION

All eukaryotic mRNAs are protected at their 5'-end by a cap structure consisting of 7-methylguanosine connected to the first transcribed nucleotide by a 5',5'-triphosphate bridge (m<sup>7</sup>GpppN; Figure 1A). Through recognition by highly specialized cap-binding proteins, the cap is involved in a number of mRNA-related processes, including maturation, nuclear export, initiation of protein synthesis and turnover (1–5). Previously, we synthesized various mRNA cap analogs in which the 5',5'-triphosphate chain was modified by substitution of either bridging O atoms (with either CH<sub>2</sub> or NH) or non-bridging O atoms (with either S or Se) (6–9). These modifications were designed to confer resistance to enzymatic cleavage of the triphosphate chain and possibly to alter other biological properties as well. The phosphate-modified cap analogs have been used to study structural requirements of cap-binding proteins and tested in biochemical assays for their enzymatic susceptibility and ability to modulate cap-dependent processes, particularly mRNA translation (10–14). These studies revealed that single-atom replacements in the triphosphate bridge can significantly influence the biological properties of the cap, both as a low molecular weight ligand and also when incorporated into synthetic mRNA.

\*To whom correspondence should be addressed. Tel: +48 22 5540774; Fax: +48 22 5540771; Email: jacekj@biogeo.uw.edu.pl

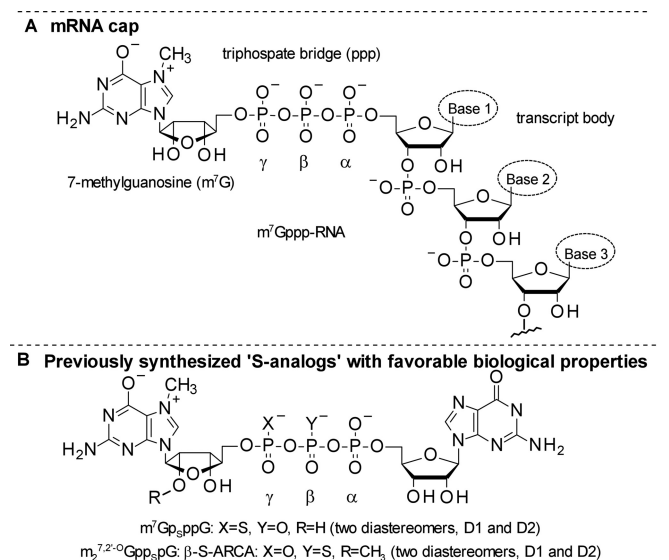
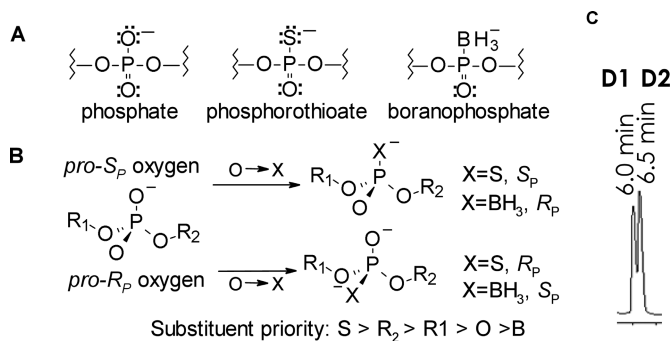


**Figure 1.** (A) Structure of the 5'-end of eukaryotic mRNA showing the cap and first three template nucleotide residues. (B) Structure of previously synthesized phosphorothioate cap analogs (S-analogs) that have favorable biological properties:  $m^7Gp_3ppG$ , a potent translational inhibitor, and  $m_2^{7,2'-O}Gpp_3pG$ , a reagent for enhancing the biological stability and translation efficiency of capped mRNAs.

The most useful analogs with single-atom modifications are the anti-reverse cap analogs (ARCAs) (15,16) containing a  $\beta$ -phosphorothioate moiety, i.e. with an O to S substitution at the  $\beta$ -phosphate of the triphosphate bridge ( $\beta$ -S-ARCA; Figure 1B) (7). RNAs capped with  $\beta$ -S-ARCA are resistant to decapping *in vitro* and have longer half-lives and higher translational efficiencies in cultured mammalian cells (10). The combination of high stability and translational efficiency makes mRNAs capped with  $\beta$ -S-ARCAs favorable for use in anticancer immunization (12). Proteins encoded by  $\beta$ -S-ARCA-capped mRNAs are expressed at up to 3-fold higher levels in immature dendritic cells compared to ARCA-capped mRNAs and elicit a greater immune response when injected into mouse lymph nodes (12).

Other useful cap analogs have a single O to S substitution at the  $\gamma$ -position of the triphosphate bridge, which makes them resistant to decapping scavenger enzymes (DcpS). DcpS enzymes remove the cap from short oligonucleotides remaining after 3'→5' mRNA degradation (17,18). The  $\gamma$ -modified analogs have also high affinity for the translational cap-binding protein eIF4E and are strong inhibitors of cap-dependent translation, which makes them potentially useful in experimental therapies that are intended to counteract elevated levels of eIF4E in cancer cells (19–21). Both their higher affinity for eIF4E and their higher stability in cell lysates make  $\gamma$ -modified analogs especially useful for targeting eIF4E (22).

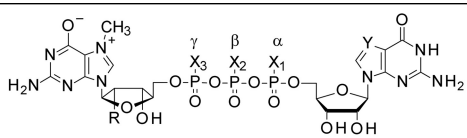
Aside from the phosphorothioates, another class of close phosphate mimics with a substitution of a non-bridging O is boranophosphates (Figure 2A). The boranophosphate and phosphorothioate moieties resemble each other in terms of structure and acid-base properties but differ in certain features that may affect their behavior in biological systems (23,24). For instance, both



**Figure 2.** Structural comparison of phosphorothioate and boranophosphate moieties. (A) Electronic structures; (B) stereochemical structures. Both O to BH<sub>3</sub> and O to S substitutions may result in P-diastereoisomerism. It should be noted, however, that the same spatial arrangement of substituents around stereogenic phosphorus center for phosphorothioate and boranophosphate groups produces different absolute configurations ( $S_P$  and  $R_P$ ) because of the different priority of BH<sub>3</sub> and S substituents according to Cahn–Ingold–Prelog priority rules. (C) A representative RP HPLC chromatogram of a mixture of two diastereomeric BH<sub>3</sub>-analogs ( $m^7Gpp_{BH_3}pG$  D1 and D2; **2a** and **2b**). D1 denotes the isomer eluting faster from a reversed-phase (RP) HPLC column.

O-to-BH<sub>3</sub> and O-to-S substitutions preserve the negative charge of the phosphate moiety under physiological pH, and both can result in P-diastereomerism (Figure 2B). In contrast to the S atom, however, the negatively charged BH<sub>3</sub> group does not have lone electron pairs and hence does not accept hydrogen bonds and interacts with metal ions poorly. This characteristic may influence the interaction of biomolecules with boranophosphate-modified nucleotides and oligonucleotides. In fact, boranophosphate-modified oligonucleotides are up to 2-fold more resistant to nucleases than phosphorothioate-modified oligonucleotides (25). Also, boranophosphate-modified oligonucleotides also exert unique reducing properties under certain conditions (26).

Because of the possibility that the boranophosphate-containing cap analogs may have different biochemical properties than their phosphorothioate-containing counterparts, we synthesized and characterized a novel series of boranophosphate cap analogs, compounds 1–6 (BH<sub>3</sub>-analogs), in which there is a single O-to-BH<sub>3</sub> substitution at either the  $\alpha$ -,  $\beta$ - or  $\gamma$ -position of the triphosphate bridge (Table 1). We analyzed conformations of the BH<sub>3</sub>-analogs and determined their interactions with two proteins that recognize free cap dinucleotides, eIF4E and DcpS. We also assessed the ability of selected new analogs to inhibit cap-dependent translation in a cell lysate as a first step in exploring their possible use as translational inhibitors in whole cells. Some of the BH<sub>3</sub>-analogs were additionally modified with a methyl group either at the 2'-O-methyl position to make them ARCAs (15–16,27) or at the N<sup>7</sup>-position of the second guanosine to make them 'two-headed' analogs (e.g.  $m^7Gppm^7G$ ) (28,29). These analogs were used to make synthetic mRNAs that were tested for protein expression in dendritic cells.

**Table 1.** Structures of novel boranophosphate cap analogs (BH<sub>3</sub>-analogs)


No <sup>[a]</sup>	Abbreviation	X <sub>1</sub>	X <sub>2</sub>	X <sub>3</sub>	R	Y
1 (a and b)	m <sup>7</sup> GpppBH <sub>3</sub> G D1 and D2	BH <sub>3</sub> <sup>-</sup>	O <sup>-</sup>	O <sup>-</sup>	OH	N
2 (a and b)	m <sup>7</sup> GppBH <sub>3</sub> pG D1 and D2	O <sup>-</sup>	BH <sub>3</sub> <sup>-</sup>	O <sup>-</sup>	OH	N
3 (a and b)	m <sup>7</sup> GpBH <sub>3</sub> ppG D1 and D2	O <sup>-</sup>	O <sup>-</sup>	BH <sub>3</sub> <sup>-</sup>	OH	N
4	m <sup>7</sup> GppBH <sub>3</sub> pm <sup>7</sup> G	O <sup>-</sup>	BH <sub>3</sub> <sup>-</sup>	O <sup>-</sup>	OH	N <sup>-</sup> -CH <sub>3</sub>
5 (a and b)	m <sub>2</sub> <sup>7,2'-O</sup> GpppBH <sub>3</sub> G D1 and D2	BH <sub>3</sub> <sup>-</sup>	O <sup>-</sup>	O <sup>-</sup>	OCH <sub>3</sub>	N
6 (a and b)	m <sub>2</sub> <sup>7,2'-O</sup> GpBH <sub>3</sub> pG D1 and D2	O <sup>-</sup>	BH <sub>3</sub> <sup>-</sup>	O <sup>-</sup>	OCH <sub>3</sub>	N

<sup>[a]</sup> **a** and **b** refer to either of the two P-diastereomers of a given compound, D1 and D2. D1 denotes the isomer eluting faster from a reversed-phased HPLC column.

## MATERIALS AND METHODS

General information on the chemical synthesis, including sources of solvents and reagents, synthesis of starting materials, diethylaminoethylene (DEAE) Sephadex chromatography, high-performance liquid chromatography (HPLC), nuclear magnetic resonance (NMR) and high-resolution mass spectrometry (HRMS) equipment and conditions are available in Supplementary file.

### 7-methylguanosine 5'-[3-(5'-guanosinyl)-1-boranotriphosphate], m<sup>7</sup>GpppBH<sub>3</sub>G (1)

To a suspension of **7** (1070 mOD, 50 mg, 0.09 mmol) and **8** (100 mg, 0.18 mmol) in 6 ml of dimethylformamide (DMF) anhydrous MgCl<sub>2</sub> (110 mg, 1.2 mmol) was added and the mixture was vigorously shaken until reagents dissolved. After stirring at room temperature (r.t.) for 10 h under microwave irradiation, the reaction was quenched by addition of 50 ml of water. The products were purified on DEAE Sephadex using 0–1.2 M gradient of triethylammonium bicarbonate (TEAB) to yield 1240 mOD (0.55 mmol, 62%) of diastereomeric mixture of **1** (triethylammonium salt). The diastereomers were separated by reversed-phase (RP) HPLC to yield 545 mOD (22 mg, 0.024 mmol, 28%) of **1a** and 450 mOD (18 mg, 0.020 mmol; 18.6%) of **1b** (both as NH<sub>4</sub><sup>+</sup> salts). MS ESI (–) *m/z* calcd. 799.1180, found 799.1195 **1a** (*R<sub>p</sub>*): δ<sub>H</sub> 9.03 (1 H, s); 8.08 (1 H, s); 5.90 (1 H, d, *J* 3.3); 5.83 (1 H, d, *J* 6.0); 4.69 (1 H, dd 6.0, 5.0); 4.58 (1 H, dd, *J* 5.0, 3.3); 4.49 (1 H, *J* 5.0, 3.2); 4.47 (1 H, *J* 5.5, 5.0); 4.40–4.20 (6 H, m); 0.38 (3 H, broad m); δ<sub>P</sub>: 84.07 (1 P, m); –11.29 (1 P, d, *J* 19.4); –22.95 (1 P, dd, *J* 19.4 Hz, *J* 30.0); **1b** (*S<sub>p</sub>*): δ<sub>H</sub>: 8.97 (1 H, s); 8.06 (1 H, s); 5.90 (1 H, d, *J* 3.0); 5.79 (1 H, d, *J* 5.7); 4.61 (1 H, m); 4.52 (1 H, m); 4.44 (2 H, m); 4.36 (2 H, m); 4.26 (4 H, m); 4.04 (3 H, m); 0.44 (3 H, m) δ<sub>P</sub>: 84.0 (1 P, m); –11.38 (1 P, d, *J* 19.5); –22.88 (1 P, dd, *J* 19.5, *J* 30.0).

### 7-methylguanosin-5'-yl-[3-(5''-guanosinyl)-2-boranotriphosphate], m<sup>7</sup>GppBH<sub>3</sub>pG (2)

To a solution of **15** (1550 mOD, 70 mg, 0.066 mmol) in 2 ml of dimethylsulfoxide (DMSO) methyl iodide (20 μl, 0.33

mmol) was added. After 3 h of stirring at r.t., the reaction was quenched by addition of 20 ml of water. The solution was adjusted to pH 7 by addition of solid NaHCO<sub>3</sub> and washed twice with 5 ml of ether. The product was purified on DEAE Sephadex using 0–1.1 M gradient of TEAB to yield 850 mOD (0.037 mmol, 56%) of **2** (triethylammonium salt). The diastereomers were separated by RP HPLC to yield 345 mOD (14.0 mg, 0.015 mmol, 23%) of **2a** and 335 mOD (13.5 mg, 0.015 mmol, 22%) of **2b** (both as NH<sub>4</sub><sup>+</sup> salts). MS ESI (–) *m/z* calcd. 799.1180, found 799.1201 **2a**: *R<sub>t</sub>* RP HPLC = 6.5 min, δ<sub>H</sub>: 8.03 (1 H, s); 5.93 (1 H, d, *J* 3.2); 5.82 (1 H, d, *J* 6.5); 4.71 (1 H, dd, *J* 6.5, 5.0); 4.56 (1 H, dd, *J* 3.2, *J* 5.0); 4.50 (1 H, dd, *J* 5.0, 3.0); 4.45 (1 H, dd, *J* 5.0, 6.0); 4.35 (3 H, m); 4.22 (3 H, m), 4.05 (3 H, s), 0.53 (3 H, m), δ<sub>P</sub>: 75.1 (1 P, m), –11.3 (2 P, ~d, *J* 30.7); **2b**: *R<sub>t</sub>* RP HPLC = 7.0 min, δ<sub>H</sub>: 8.96 (1 H, s); 8.02 (1 H, s); 5.91 (1 H, d, *J* 3.2); 5.81 (1 H, d, *J* 6.5); 4.70 (1 H, dd, *J* 6.5, 4.9); 4.56 (1 H, dd, *J* 5.0, 3.2); 4.50 (1 H, dd, *J* 4.9, 3.0); 4.45 (1 H, dd, *J* 6.0, 5.0); 4.35 (3 H, m); 4.22 (3 H, m), 4.05 (3 H, s); 0.53 (3 H, m), δ<sub>P</sub>: 75.13 (1 P, m) –11.31 (2P, ~d, *J* 30.7).

### 7-dimethylguanosine 5'-[3-(5'-guanosinyl)-3-boranotriphosphate], m<sup>7</sup>GpBH<sub>3</sub>ppG (3)

Obtained analogously to **1** starting from **13** (915 mOD, 65 mg, 0.080 mmol), **14** (1320 mOD, 60 mg, 0.22 mmol) and MgCl<sub>2</sub> (220 mg, 2.3 mmol) in 3 ml of DMF. The reaction was quenched after 2 h by addition of 20 ml of water. The products were separated by DEAE Sephadex using 0–1.2 M gradient of TEAB to yield 1480 mOD (0.66 mmol, 81%) of diastereomeric mixture of **3**. The diastereomers were separated using RP HPLC to yield 690 mOD (28 mg, 0.031 mmol, 38%) of **3a** and 570 mOD (22 mg, 0.025 mmol; 23%) of **3b** (both as NH<sub>4</sub><sup>+</sup> salts). MS ESI (–) *m/z* calcd. 799.1180, found 799.1198 **3a** (*S<sub>p</sub>*): δ<sub>H</sub> 8.92\* (1 H, s); 8.01 (1 H, s); 5.85 (1 H, d, *J* 2.5); 5.79 (1 H, d, *J* 6.2); 4.66 (1 H, dd, *J* 6.2, 5.0); 4.48 (2 H, m); 4.38–4.22 (7 H, m); 4.08 (3 H, s, CH<sub>3</sub>); 0.42 (3 H, broad m), δ<sub>P</sub> 84.5 (1 P, m); –11.52 (1 P, m); –23.03 (1 P, m); **3b** (*R<sub>p</sub>*): δ<sub>H</sub>: 9.02\* (1 H, s); 8.04 (1 H, s); 5.97 (1 H, d, *J* 3.2); 5.83 (1 H, d, *J* 6.0); 4.70 (1 H, dd, *J* 6.0, 5.0); 4.61 (1 H, dd, *J* 4.8, 3.2); 4.52 (1 H, dd, *J* 6.2, 4.8); 4.50 (1 H, dd, *J* 5.0, 3.5); 4.39 (1H, m); 4.35–4.22 (5H, m); 4.07 (3H, s); 0.41 (3H, broad m) δ<sub>P</sub>: 84.2 (1 P, m); –11.37 (1 P, m); –23.05 (1 P, m).

### bis(7-methylguanosin-5',5''-yl) (2-boranotriphosphate), m<sup>7</sup>GppBH<sub>3</sub>pm<sup>7</sup>G (4). Method I

Obtained analogously as **2** starting from GppBH<sub>3</sub>pG (2200 mOD, 100 mg, 0.092 mmol) and 60 μl (0.1 mmol) of methyl iodide in 3 ml of DMSO. The reaction was quenched after 4 h by addition of 30 ml of water. The product was purified on DEAE Sephadex using a 0–1.1 M gradient of TEAB. After evaporation, m<sup>7</sup>GppBH<sub>3</sub>pm<sup>7</sup>G triethylammonium salt was converted into sodium salt on Dowex 50 Wx8 (200–400 mesh, sodium form) to yield, after repeated freeze-drying, 990 mOD of **4** sodium salt (40 mg, 0.045 mmol, 48%).

### Method II

Compound **16** (Na salt, 63 mg, 1390 mOD, 0.120 mmol) was mixed with boranophosphate (TEA salt, 70 mg, 0.120

mmol) and  $\text{MgCl}_2$  (8 eq, 105 mg, 1.12 mmol) and dissolved in DMF (1 ml) under stirring. Reaction was monitored by RP HPLC. After 2.5 h, the reaction was quenched by addition of MQ water (10 ml). The product was purified on DEAE Sephadex using 0–1 M linear gradient of TEAB in water to afford 400 mOD (0.017 mmol, 57%) of **4**, triethylammonium salt. Subsequent conversion into ammonium salt on semi-preparative RP HPLC and repeatedly freeze-drying resulted with 6.0 mg of **4**. MS ESI (–)  $m/z$  calcd. 813.1336, found 813.1357;  $R_t$  RP HPLC = 8.4 min,  $\delta_H$ : 9.15\* (2H, s); 6.03 (2H, d,  $J$  3.7); 4.65 (2H, m); 4.52 (2H, m); 4.40 (2H, m); 4.34 (2H, m); 4.22 (2H, m); 4.12 (6H, s); 0.44 (3H, m),  $\delta_P$ : 74.90 (1P, m), –11.33 (1P, d,  $J$  31.0), –11.36 (1P, d,  $J$  31.0).

**2'-O,7-dimethylguanosine 5'-[3-(5'-guanosinyl)-3-boranotriphosphate],  $m^7,2'-O\text{GpppBH}_3\text{G}$  (**5**)**

Obtained analogously as **1** starting from **7** (1320 mOD, 60 mg, 0.11 mmol) and **9** (120 mg, 0.22 mmol) and  $\text{MgCl}_2$  (160 mg, 1.7 mmol) in 6 ml of DMF. The products were separated on DEAE Sephadex using 0–1.2 M gradient TEAB to yield 1450 mOD (0.64 mmol, 60%) of diastereomeric mixture of **5**. The diastereomers were separated by RP HPLC to yield 700 mOD (28 mg, 0.031 mmol, 28%) of D1 and 465 mOD (19 mg, 0.020 mmol; 18.6%) of D2 (both as  $\text{NH}_4^+$  salts). MS ESI (–)  $m/z$  calcd. 813.1336, found 813.1361; **5a** ( $R_P$ ):  $R_t$  RP HPLC = 7.1 min;  $\delta_H$  9.02\* (1 H, s); 8.08 (1 H, s); 5.94 (1 H, d,  $J$  2.7); 5.83 (1 H, d,  $J$  6.0); 4.69 (1 H, dd,  $J$  6.0, 5.1); 4.55 (1 H, dd, 6.0, 5.2); 4.50 (1 H, dd,  $J$  5.1, 3.5); 4.40 (1 H, m); 4.35–4.22 (6H, m); 4.07 (3H, s); 3.59 (3H, s), 0.40 (3H, m);  $\delta_P$ : 83.7 (1 P, m), –11.30 (1 P, d,  $J$  19.5); –22.91 (1 P, dd,  $J$  19.5 Hz,  $J$  30.0); **5b** ( $S_P$ ):  $R_t$  RP HPLC = 7.8 min,  $\delta_H$  8.97 (1 H, s); 8.05 (1 H, s); 5.95 (1 H, d,  $J$  2.7); 5.78 (1 H, d,  $J$  6.0); 4.61 (1 H, dd,  $J$  6.0, 5.0); 4.49 (1 H, dd,  $J$  6.0, 5.0); 4.45 (1 H, dd,  $J$  5.0, 3.5); 4.34–4.18 (7H, m); 4.05 (3H, s); 3.60 (3H, s), 0.40 (3H, m),  $\delta_P$ : 83.7 (1 P, m), –11.41 (1 P, d,  $J$  19.0); –22.87 (1 P, dd,  $J$  19.0, 32.0).

**P1-7,2'-O-dimethylguanosin-5'-yl P3-guanosine-5'-yl (2-boranotriphosphate), ammonium salt,  $m_2^{7,2'-O}\text{GpppBH}_3\text{pG}$  (**6**)**

Compound **17** (330 mOD, 15 mg, 0.029 mmol) and boranophosphate triethylammonium salt (30 mg, 0.15 mmol) were mixed in 1 ml of DMF followed by addition of  $\text{MgCl}_2$  (40 mg, 0.40 mmol) and left under stirring for 1–2 min. Subsequently, **14** (940 mOD, 40 mg, 0.078 mmol) and  $\text{MgCl}_2$  (40 mg, 0.40 mmol) were added under stirring. After 5 h, the reaction was quenched by addition of water (20 ml). The product was purified on DEAE Sephadex using 0–1.2 M linear gradient of TEAB to afford 280 mOD (0.012 mmol, 41%) of **6** triethylammonium salt. Diastereoisomers D1 and D2 were then separated on semi-preparative RP HPLC and, after repeated freeze-drying, isolated as ammonium salts (D1, **6a**, 125 mOD, 5.1 mg, 0.0053 mmol, 19%) (D2, **6b**, 120 mOD, 4.8 mg, 0.0056 mmol, 18%). MS ESI (–)  $m/z$  calcd. 813.1336, found 813.1372; **6a**:  $R_t$  RP HPLC = 7.9 min;  $\delta_H$ : 8.98 (1 H, s); 8.03 (1 H, s); 5.98 (1 H, d,  $J$  2.5); 5.81 (1 H, d,  $J$  6.2); 4.67 (1 H, dd,  $J$  6.2, 5.0); 4.51 (1 H, dd,  $J$  6.0, 5.0); 4.49 (1 H, dd,  $J$  5.0, 3.5); 4.38 (1 H, m); 4.35–4.30

(2H, m); 4.27 (2H, m); 4.23 (4H, m); 4.06 (3H, s); 3.61 (3H, s), 0.45 (3H, m),  $\delta_P$ : 75.12 (1 P, m), –11.09 (2P, d,  $J$  30.7), **6b**:  $R_t$  RP HPLC = 8.3 min;  $\delta_H$ : 8.97 (1 H, s); 8.05 (1 H, s); 5.95 (1 H, d,  $J$  2.5); 5.78 (1 H, d,  $J$  6.2); 4.61 (1 H, dd,  $J$  6.2, 4.8); 4.49 (1 H, dd,  $J$  6.0, 5.0); 4.44 (1 H, dd,  $J$  5.0, 3.5); 4.36–4.18 (7H, m); 4.05 (3H, s); 3.60 (3H, s), 0.45 (3H, m),  $\delta_P$ : 75.12 (1 P, m), –11.11 (2P, ~d,  $J$  30.7).

**7-methylguanosine 5'-(1-boranodiphosphate),  $m^7\text{GDP}\alpha\text{BH}_3$  (**13**)**

To a solution of  $\text{GDP}\alpha\text{BH}_3$  (2075 mOD, 0.17 mmol) in 3.45 ml of DMSO  $\text{CH}_3\text{I}$  (85  $\mu\text{l}$ ) was added and the solution was kept at r.t. under stirring for 2.5 h. The reaction was quenched by addition of 35 ml of water, adjusted to pH 6 with solid  $\text{NaHCO}_3$  if necessary, and repeatedly extracted by diethyl ether. The product was purified by DEAE Sephadex using 0–0.9 M gradient of TEAB to yield 1360 mOD (0.12 mmol, 70%) of  $m^7\text{GDP}\alpha\text{BH}_3$  diastereomeric mixture.  $R_t$  RP HPLC = 5.0 min; MS ESI (–)  $m/z$  calcd. 454.0706, found 454.0765; **13a**:  $R_t$  RP HPLC = 5.0 min;  $\delta_H$  9.20 (1 H, s); 6.07 (1 H, d,  $J$  3.4); 4.68 (1 H, dd,  $J$  4.5, 3.4); 4.47 (1 H, dd,  $J$  5.5, 4.5); 4.44 (1 H, m); 4.28 (2 H, m); 4.16 (3 H, s); 0.40 (3 H, m);  $\delta_P$  75.12 (1 P, m), –11.09 (2 P, d,  $J$  30.7), **13b**:  $R_t$  RP HPLC = 5.5 min;  $\delta_H$  9.11 (1 H, s); 6.07 (1 H, d,  $J$  3.2); 4.69 (1 H, dd,  $J$  4.6, 3.2); 4.56 (1 H, dd,  $J$  5.8, 4.6); 4.42 (1 H, m); 4.25 (2H, m); 4.15 (3H, s); 0.40 (3H, m),  $\delta_P$  75.12 (1 P, m), –11.11 (2 P, ~d,  $J$  30.7),  $\delta_P$  81.9 (1 P, d,  $J$  32.0), –10.32 (1 P, d,  $J$  32.0).

**Diguanosine 5',5'-(2-boranotriphosphate),  $\text{GpppBH}_3\text{pG}$  (**15**)**

To a mixture of **14** (4700 mOD, 200 mg, 0.39 mmol) and triethylammonium boranophosphate (70 mg, 0.23 mmol) suspended in 5 ml of DMF anhydrous  $\text{MgCl}_2$  (380 mg, 4.0 mmol) was added and left at r.t. under stirring for 1 h. The reaction was quenched by addition of 50 ml of water. The product was purified on DEAE Sephadex using 0–1.2 M gradient of TEAB to yield 3760 mOD (170 mg, 0.16 mmol, 80%) of **15** triethylammonium salt.  $R_t$  RP HPLC = 6.2 min MS ESI (–)  $m/z$  calcd. 785.1023 found 785.1097,  $\delta_H$  8.10 (1 H, s); 8.08 (1 H, s); 5.83 (2 H, d,  $J$  5.2); 4.68 (2 H, t,  $J$  5.2); 4.49 (2 H, m); 4.30 (2 H, m); 4.23 (4H, m);  $\delta_P$  75.10 (1 P, m), –11.20 (1 P, dt,  $J$  30.2, 5.0), –11.28 (1 P, dt,  $J$  30.2, 5.0).

**Adenosine 5'-(1-borano-2-imidazolyl-diphosphate), dilithium salt (**20**)**

Compound **19** (2 060 mOD, 90 mg, 0.137 mmol, 4:5  $R_P/S_P$  diastereomeric mixture) was mixed with imidazole (93 mg, 1.36 mmol), 2,2'-dithiodipiridine (91 mg, 0.414 mmol), DMF (2 ml) and triethylamine 57  $\mu\text{l}$ . The suspension was stirred for 5 min followed by addition of triphenylphosphine (108 mg, 0.412 mmol) and left under stirring at r.t. for 4 h (complete dissolution of reagents was observed during first 10 min). The product was precipitated as a lithium salt by pouring the reaction mixture into  $\text{LiClO}_4$  (140 mg) solution in acetonitrile (ACN) (50 ml). The product was centrifuged, supernatant discarded. The pellet was repeatedly washed with cold acetonitrile by re-suspension/centrifugation. After drying under reduced pressure over  $\text{P}_2\text{O}_5$  1700 mOD (84

mg, 0.113 mmol, 83%) of compound **20** ( $S_P/R_P$  diastereomeric mixture) were isolated as a white powder. RP HPLC  $R_t$ : 9.0 min (D1) and 9.5 min (D2); MS ESI (-)  $m/z$  = 474.1.

#### Diadenosine 5',5'-(1,3-diboranotriphosphate), $Ap_{BH_3}PP_{BH_3}A$ (**21**)

Obtained analogously as **1** starting from **18** (620 mOD, 20 mg, 0.041 mmol), **20** (410 mOD, 20 mg, 0.027 mmol) and  $MgCl_2$  (78 mg, 0.82 mmol) in 2 ml DMF. The reaction was quenched after 5 days by diluting with 10 ml of water. The products were purified on DEAE Sephadex using 0–1.2 M gradient of TEAB to yield 495 mOD (0.020 mmol, 70%) of diastereomeric (**21a**:**21b**:**21c** ratio 10:20:15 by HPLC) mixture of **21**. The diastereomers were partially resolved by RP HPLC to yield 335 mOD (8.5 mg, 0.013 mmol, 48%) of **21a,b** (8:20) and 170 mOD (0.0066 mmol, 3.6 mg, 24%) of **21c**. MS ESI(-)  $m/z$ : calcd. 751.1504 found. 751.1543; **21a** ( $R_P, R_P$ ):  $R_t$  RP HPLC = 9.7 min,  $\delta_H$  8.51 (2 H, s); 8.22 (2 H, s); 6.09 (2 H, d,  $J$  5.0); 4.75 (2 H, t,  $J$  5.0); 4.66 (2 H, dd,  $J$  5.0, 4.0); 4.38 (2 H, m); 4.29 (4 H, m); 0.48 (3 H, m);  $\delta_P$  82.5 (2 P, m), -22.6 (1 P, m); **21b** ( $R_P, S_P$ ):  $R_t$  RP HPLC = 9.9 min;  $\delta_H$  8.48 (1 H, s); 8.44 (1 H, s); 8.19 (1 H, s); 8.19 (1 H, s); 6.04 (1 H, d,  $J$  5.2); 6.01 (1 H, d,  $J$  5.2); 4.60 (1 H, dd,  $J$  5.2, 5.0); 4.64 (1 H, dd,  $J$  5.2, 5.0); 4.56 (1 H, dd,  $J$  5.0, 3.7); 4.49 (1 H, dd,  $J$  5.0, 4.0); 4.38 (2 H, m); 4.29 (4 H, m); 0.48 (3 H, m);  $\delta_P$  82.5 (2 P, m), -22.6 (1 P, m); **21c** ( $S_P, S_P$ ):  $R_t$  RP HPLC = 11.6 min  $\delta_H$  8.45 (2 H, s); 8.16 (2 H, s); 6.01 (2 H, d,  $J$  5.2); 4.60 (2 H, dd,  $J$  5.2, 4.8); 4.45 (2 H, dd,  $J$  4.8, 3.2); 4.40 (2 H, m); 4.33 (4 H, m); 0.48 (3 H, m);  $\delta_P$  82.5 (2 P, m), -22.6 (1 P, m).

#### Pyrophosphate P1,P2-bis(phosphorimidazolide), disodium salt (**22**)

Pyrophosphate (triethylammonium salt, 1084 mg, 2.84 mmol) was mixed with imidazole (3870 mg, 56.8 mmol), 2',2'-dithiodipiridine (2840 mg, 14.2 mmol), DMF (16 ml) and triethylamine (0.8 ml). The suspension was stirred for 30 min followed by addition of triphenylphosphine (3720 mg, 14.2 mmol) and left under stirring for 18 h. The product was precipitated as a sodium salt by pouring the reaction mixture into  $NaClO_4$  (2430 mg) solution in ice-cold acetone (80 ml). The product was left for 4 h at 4°C and centrifuged, supernatant discarded. The pellet was repeatedly washed with cold acetone by resuspension/centrifugation. After drying under reduced pressure over  $P_2O_5$  887 mg (97%, 2.75 mmol) of compound **22** were isolated as a white powder.

#### Guanosine 5'-O-(1-borano)triphosphate, triethylammonium salt, $GTP\alpha BH_3$ (**23**)

Compound **20** (sodium salt, 256 mg, 0.8 mmol) and anhydrous  $MgCl_2$  (380 mg, 4 mmol) were mixed in anhydrous DMF (10 ml) followed by addition of compound **7** (triethylammonium salt, 2400 mOD, 92 mg, 0.2 mmol). After 48 h reaction was quenched by addition of 90 ml of water. The product was purified on DEAE Sephadex using 0–1.4 M linear gradient of TEAB in water and isolated as triethylammonium salt (1055 mOD, 0.088 mmol, 44%). Diastereoisomers,

D1 (**23a**) and D2 (**23b**) (125 mOD), were then separated on semi-preparative RP HPLC and, after repeated freeze-drying, isolated as ammonium salts (D1: 52 mOD, 0.0044 mmol, 2.5 mg; D2: 42 mOD., 0.0035 mmol, 2 mg). MS ESI (-)  $m/z$  calcd. 520.0212, found 520.0223; **23a** ( $R_P$ ):  $\delta_H$  8.20 (1 H, s); 5.95 (1 H, d,  $J$  6.0); 4.81 (1 H, d,  $J$  6.0); 4.62 (1 H, d,  $J$  2.5); 4.37 (1 H, d,  $J$  2.5); 4.29 (1 H, m); 4.16 (1 H, m); 0.47 (3 H, m);  $\delta_P$  83.93 (1 P, d,  $J$  29.3); -10.34 (1 P, d,  $J$  16.5 Hz); -22.96 (1 P, dd,  $J$  29.3, 16.5 Hz); **23b** ( $S_P$ ):  $\delta_H$  8.18 (1 H, s); 5.94 (1 H, d,  $J$  5.1); 4.82 (1 H, dd,  $J$  5.1, 3.4); 4.54 (1 H, dd,  $J$  3.4, 2.5); 4.37 (1 H, d,  $J$  2.5); 4.24 (2 H, m); 0.43 (3 H, m);  $\delta_P$  83.40 (1 P, d,  $J$  34.4); -10.50 (1 P, d,  $J$  22.4); -22.95 (1 P, dd,  $J$  34.4, 22.4).

#### Adenosine 5'-O-(1-boranotriphosphate), $ATP\alpha BH_3$ (**24**)

Compound **18** (TEA salt, 3200 mOD, 60 mg, 0.21 mmol) and compound **22** (Na salt, 80 mg, 0.25 mmol) were mixed in anhydrous DMF (2 ml) followed by addition of anhydrous  $MgCl_2$  (513 mg, 5.4 mmol). After 24 h reaction was quenched by addition of MQ water (90 ml). The product was purified on DEAE Sephadex using 0–1.12 M linear gradient of TEAB in water and isolated as TEA salt (1660 mOD, 0.11 mmol, 52%). Diastereoisomers D1 (**24a**) and D2 (**24b**) (500 mOD) were then separated on semi-preparative RP HPLC and, after repeated freeze-drying, isolated as ammonium salts (**24a**: 135 mOD., 0.0090 mmol, 9 mg; **24b**: 75 mOD., 0.0050 mmol, 5.5 mg). MS (ESI-)  $m/z$  ( $M-H^+$ ) calc. 504.0263, found 504.0286; **24a**:  $R_t$  = 5.2 min;  $^1H$  NMR  $\delta_H$  8.64 (1 H, s), 8.33 (1 H, s), 6.17 (1 H, d,  $J$  5.5), 4.80 (1 H, dd,  $J$  5.5, 4.9), 4.63 (1 H, dd,  $J$  4.9, 3.6), 4.42 (1 H, dt,  $J$  3.6, 3.0), 4.16 (1 H, ddd,  $J$  12.0, 7.0, 3.0), 4.05 (1 H, ddd,  $J$  12.0, 4.9, 3.0), 0.46 (3 H, m);  $\delta_P$  84.31 (1 P, m), -10.75 (1 P, d,  $J$  19.5), -22.88 (1 P, dd,  $J$  30.0, 19.5); **24b**:  $\delta_H$  8.58 (1 H, s), 8.27 (1 H, s), 6.15 (1 H, d,  $J$  5.7), 4.78 (1 H, dd,  $J$  5.7, 5.0), 4.56 (1 H, dd,  $J$  5.0, 3.5 Hz), 4.42 (1 H, dt,  $J$  3.5, 3.0), 4.26 (1 H, ddd,  $J$  12.0, 7.0, 3.0), 4.21 (1 H, ddd,  $J$  12.0, 4.9, 3.0), 0.44 (3 H, m);  $\delta_P$  81.38–86.79 (1 P, m), -9.84 (1 P, d,  $J$  16.6), -22.51 (1 P, dd,  $J$  30.0, 16.6).

#### Stacking measurements

The population of the stacked dinucleotide cap analogs was determined comparing its fluorescence intensity to fluorescence intensity of  $m^7GMP$  in 50 mM phosphate buffer (pH 5.2) at  $20.0 \pm 0.3^\circ C$  according to the equation (30):

$$\%_{\text{stacking}} = \frac{[\text{stacked}]}{[\text{unstacked}] + [\text{stacked}]} = \frac{F_{(m^7GMP)} - F_{(\text{cap})}}{F_{(m^7GMP)}}$$

#### Molecular modeling

Molecular dynamics simulations were performed with the Desmond package as implemented in the Maestro Suite from Schrödinger. All parameters, including partial charges of mononucleotides, were assigned from an OPLS2005 force-field. Each mononucleotide was solvated in a cubic box filled with Simple Point Charge (SPC) water molecules. Systems were heated and equilibrated with the standard Desmond Maestro protocol. All simulations were run in NPT ensemble with Nose–Hoover thermal bath (coupling

time 1.0 ps,  $T = 300$  K) and Martyna–Tobias–Klein pressure coupling (coupling time 2.0 ps,  $P = 1$  atm). Equations of motion were integrated numerically with a multiple time-step RESPA algorithm. Bonded and near non-bonded interactions were computed every 2.0 fs and far non-bonded interactions were integrated every 6.0 or 9.0 fs. A cutoff was applied to electrostatic interactions and particle-mesh Ewald summation was applied for particles placed beyond this distance. The snapshots were recorded every 4.8 ps.

### Preparation of recombinant proteins

Mouse eIF4E (residues 28–217) was expressed in *Escherichia coli* strain BL21(DE3) as inclusion bodies. Guanidinium-solubilized protein was refolded by one-step dialysis, and purified by ion-exchange chromatography on HiTrap SP column (GE Healthcare) without exposure to cap analogs. The concentration of eIF4E was determined spectrophotometrically ( $\epsilon_{280} = 53\,400\text{ cm}^{-1}\text{ M}^{-1}$ ). *Caenorhabditis elegans* DcpS (CeDcpS) was expressed in *E. coli* with a pET16b vector as described previously (31). The protein was purified on a nickel-nitrilotriacetic acid (Ni-NTA)-affinity column under native conditions. The concentration of CeDcpS was determined spectrophotometrically ( $\epsilon_{280} = 38\,900\text{ cm}^{-1}\text{ M}^{-1}$ ).

### HPLC-based assays of DcpS-mediated hydrolysis

Two assays were used to measure the products of digestion with either human or *C. elegans* DcpS.

*Assay 1 (lower enzyme concentration)*. Assays were performed in 50 mM Tris HCl pH 7.9, 20 mM MgCl<sub>2</sub> and 60 mM (NH<sub>4</sub>)<sub>2</sub>SO<sub>4</sub>, at 30°C. DcpS enzyme concentration was 0.1 μM, while the initial substrate concentration was 40 μM. Samples of 100 μl were collected from the reaction mixtures after 15 min, 30 min, 1 h and 2 h. The enzyme was heat-inactivated by incubation at 98°C for 2 min followed by cooling on ice. The samples were analyzed by analytical RP HPLC as described in Supplementary file.

*Assay 2 (higher enzyme concentration)*. Assays were performed in 50 mM Tris HCl, 200 mM KCl, 0.5 mM ethylenediaminetetraacetic acid (EDTA) and 1 mM dithiothreitol (DTT) (final pH 7.6), at 20°C by HPLC. DcpS enzyme concentration was 0.2 μM (the same as in the binding studies), while the initial substrate concentration was 15 μM. Before the enzyme addition, 1 ml of buffer solution containing the investigated cap analog was maintained at 20°C for 10 min. The reaction was started by the enzyme addition and was stopped at 10 and 90 min by heat inactivation of the sample (200 μl aliquot of the reaction mixture) at 97°C for 2.5 min. The mobile phase for analytical RP HPLC analysis was a linear gradient of methanol from 0% to 30% in aqueous 0.1 M KH<sub>2</sub>PO<sub>4</sub>, at a flow rate of 1.3 ml/min, over 15 min) at room temperature. For quantitative comparison of enzyme activity toward various cap analogs studied we further determined the extent of decapping ( $x$ ) measured as the percentage of hydrolyzed substrate.

### Fluorescence assays

Fluorescence titration measurements were carried out on an LS-55 spectrofluorometer (Perkin Elmer Co.) in a quartz cuvette (Hellma) with an optical path length of 4 mm for absorption and 10 mm for emission. The eIF4E measurements were performed in 50 mM HEPES/KOH (pH 7.2), 100 mM KCl, 0.5 mM EDTA and 1 mM DTT, and the DcpS measurements in 50 mM Tris HCl, 200 mM KCl, 0.5 mM EDTA and 1 mM DTT (final pH 7.6), both at 20.0 ± 0.3°C. Aliquots of 1 μl increasing concentration of cap analog solutions were added to 1.4 ml of 0.1 μM eIF4E solutions or 0.2 μM DcpS solutions. Fluorescence intensities (excitation at 280 nm with 2.5-nm bandwidth and detection at 340 nm with 4 nm bandwidth and 290 nm cut-off filter) were corrected for sample dilution and the ‘inner filter’ effect. Equilibrium association constants ( $K_{AS}$ ) were determined by fitting the theoretical dependence of the fluorescence intensity on the total concentration of cap analog to the experimental data points as described previously (32). The final  $K_{AS}$  was calculated as a weighted average of three to five independent titration assays. Numerical non-linear least-squares regression analysis was performed using ORIGIN 6.0 (Microcal Software Inc., USA). The Gibbs free energy of binding was calculated from the  $K_{AS}$  value according to the standard equation  $\Delta G^0 = -RT\ln K_{AS}$ .

### Inhibition of translation by cap analogs in rabbit reticulocyte lysate system

Inhibition experiments of cap-dependent translation in RRL (rabbit reticulocyte lysate; Flexi Rabbit Reticulocyte Lysate System, Promega) by cap analogs, evaluation of their stability in RRL lysate and determination of IC<sub>50</sub> values were performed as described previously (8). Briefly, the *in vitro* translation reactions (12.5 μl total volume) contained a tested cap analog (inhibitor) at a concentration falling in the range of 0 to 50 μM and m<sub>2</sub><sup>7,3'-O</sup>GpppG-capped reporter luciferase mRNA at 5 μg/ml. Two variants of the experiment (A and B) were performed in order to evaluate the susceptibility of tested cap analogs to degradation in RRL and its correlation to inhibitory properties. In ‘experimental setup A’, the RRL was pre-incubated at 30°C for 60 min and, then, the cap analog and luciferase mRNA were added at the same time. In ‘experimental setup B’ the cap analog was pre-incubated in RRL at 30°C for 60 min, followed by addition of luciferase mRNA. All reactions were stopped 60 min after addition of mRNA by chilling on ice and the luciferase activity was measured in a luminometer (Glomax, Promega). It was confirmed in a separate experiment that a linear increase in luciferase activity was observed when luciferase mRNA was translated in RRL over the period of 60 min, similarly as described previously (8).

### mRNA expression in dendritic cells

Luciferase-encoding mRNAs were prepared by *in vitro* transcription with T7 RNA polymerase as described before (12). By adding the respective cap di-nucleotide to the reaction solution it is incorporated co-transcriptionally forming the 5'-end of the RNA. Following enzymatic digestion of plasmid DNA, the RNA was purified using mag-

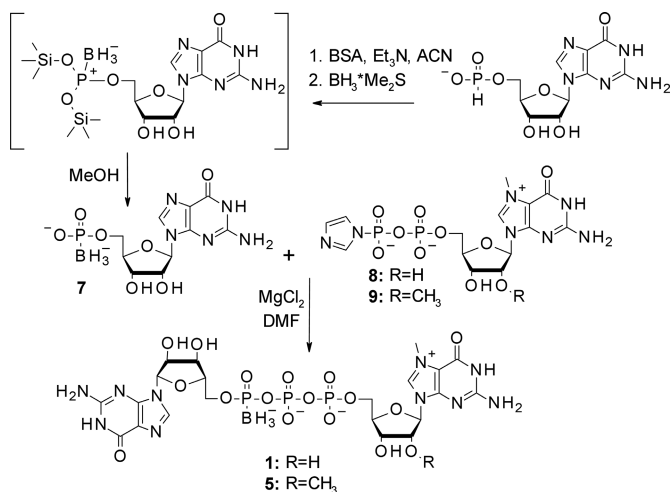


**Figure 3.** Synthesis of cap BH<sub>3</sub>-analogs **1** and **5** modified at the  $\alpha$ -position of the triphosphate bridge. Abbreviations—BSA: *N,O*-bis(trimethylsilyl)acetamide; ACN: acetonitrile.

netic beads (Dynabeads MyOne carboxylic acid, Invitrogen, Carlsbad, CA, USA) (**33**) and was finally stored in water. RNA concentrations were measured by ultraviolet absorption at 260 nm (Nanodrop 1000, Thermo Scientific, Wilmington, DE, USA) and RNA integrity was verified by microfluidics-based electrophoreses (2100 Bioanalyzer, Agilent Technologies, Inc., Santa Clara, CA, USA). For differentially 5'-capped RNAs, no significant differences in RNA integrity could be observed. Luciferase expression in human immature dendritic cells (hiDCs) was monitored at different time points (2, 4, 8, 24, 48 and 72 h) following electroporation of differentially 5'-capped mRNAs (for experimental details, see (**12**)). Luciferase activity was normalized against cell numbers and depicted as a function of time (Figure 5) and further analysis was performed by spline interpolation of the experimental data points as described, using the R software (R Development Core Team, 2008) resulting in functional parameters summarized in Table 8.

## RESULTS

### Synthesis and characterization of cap BH<sub>3</sub>-analogs

**Chemical synthesis.** The chemical synthesis of BH<sub>3</sub>-analogs **1–6** was based on phosphorimidazole chemistry and boranophosphate-containing nucleotides as nucleophiles (Figures 3–5). For all the compounds shown, several routes and reaction conditions were tested to select the ones that were most efficient and potentially suitable for up-scaling. As a starting point, we chose conditions that had proven to be effective for the synthesis of S-analogs, i.e. coupling a nucleoside phosphorimidazole with a modified-phosphate-bearing nucleophile in DMF in the presence of ZnCl<sub>2</sub> excess (**7,38**). However, we found that the optimal conditions for the synthesis of boranophosphate cap analogs are different because of different chemical properties and stability of the boranophosphate nucleotides. The synthesis of cap analog **1** modified at the  $\alpha$ -position of the triphosphate bridge was attempted by coupling of guanosine 5'-monoboranophosphate (**7**) with a 7-

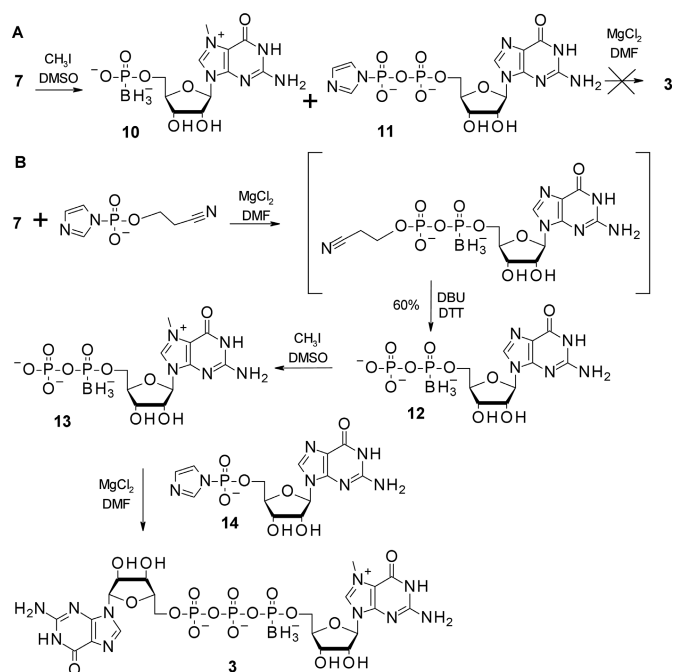


**Figure 4.** Synthetic routes for cap BH<sub>3</sub>-analog modified at the  $\gamma$ -position of the triphosphate bridge (**3**). (A) Attempted synthesis by coupling of 7-methylguanosine 5'-boranophosphate (**10**) and GDP imidazole derivative. (B) A successful approach employing 7-methylguanosine 5'-(1-boranodiphosphate) (**13**) as the key intermediate.

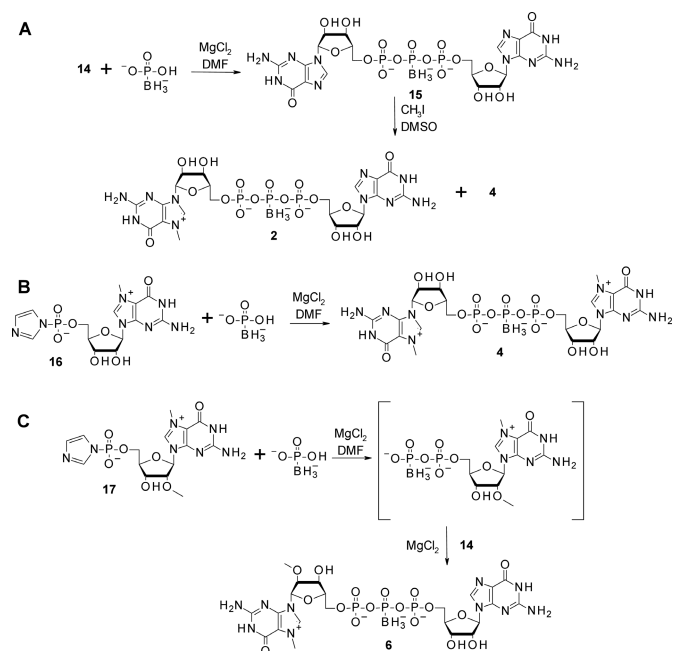


**Figure 5.** Synthesis of cap BH<sub>3</sub>-analogs **2** (A), **4** (B) and **6** (C) modified at the  $\beta$ -position of the triphosphate bridge.

methylguanosine diphosphate P-imidazole derivative (**8**). First, **7** was synthesized from guanosine 5'-H-phosphonate via boronation of a trimethylsilylated intermediate (Figure 3) (**39**). Although the conversion was almost quantitative, the isolated yield was only 60% because of par-

**Table 2.** Selected <sup>1</sup>H NMR data for α- and γ-modified cap analogs and corresponding nucleoside 5'-diphosphates

No.	Compound	Absolute config.	δ <sub>H8</sub> <sup>a</sup> (ppm)	δ <sub>H1'</sub> <sup>a</sup> (ppm)	δ <sub>H3'</sub> <sup>a</sup> (ppm)	Δδ <sub>H8</sub> (RP-SP) <sup>a</sup>	Δδ <sub>H3'</sub> (RP-SP) <sup>a</sup>	BH <sub>3</sub> -H3' distance (Å) <sup>b</sup>
<b>1a</b>	m <sup>7</sup> GpppBH <sub>3</sub> G D1	<i>R<sub>P</sub></i>	8.08	5.83	4.48	0.02	0.04	n.d.
<b>1b</b>	m <sup>7</sup> GpppBH <sub>3</sub> G D2	<i>S<sub>P</sub></i>	8.06	5.79	4.44			n.d.
<b>3a</b>	m <sup>7</sup> GpBH <sub>3</sub> ppG D1	<i>S<sub>P</sub></i>	8.92	5.85	4.47	0.10	0.03	n.d.
<b>3b</b>	m <sup>7</sup> GpBH <sub>3</sub> ppG D2	<i>R<sub>P</sub></i>	9.02	5.97	4.50			n.d.
<b>5a</b>	m <sub>2</sub> <sup>7,2'-O</sup> GpppBH <sub>3</sub> G D1	<i>R<sub>P</sub></i>	8.08	5.83	4.50	0.03	0.06	n.d.
<b>5b</b>	m <sub>2</sub> <sup>7,2'-O</sup> GpppBH <sub>3</sub> G D2	<i>S<sub>P</sub></i>	8.05	5.78	4.44			n.d.
<b>12a</b>	GDPαBH <sub>3</sub> D1	<i>R<sub>P</sub></i>	8.20	5.95	4.59	0.02	0.07	6.70 ± 0.02
<b>12b</b>	GDPαBH <sub>3</sub> D2	<i>S<sub>P</sub></i>	8.18	5.95	4.52			6.04 ± 0.09
<b>13a</b>	m <sup>7</sup> GDPαBH <sub>3</sub> D1	<i>S<sub>P</sub></i>	9.20	6.07	4.47	-0.08	0.09	5.68 ± 0.17
<b>13b</b>	m <sup>7</sup> GDPαBH <sub>3</sub> D2	<i>R<sub>P</sub></i>	9.11	6.07	4.56			6.4 ± 0.2

<sup>a</sup>400 MHz, 25°C, D<sub>2</sub>O referred to TSP.<sup>b</sup>Average BH<sub>3</sub>-H3' distances were calculated by molecular dynamics simulations as described in the Materials and Methods section and are shown as mean ± SD.**Table 3.** Intermolecular base-stacking of cap analogs 1–3

Dinucleotide	% of stacked conformation <sup>a</sup>	
	<i>X</i> = BH <sub>3</sub>	<i>X</i> = S
m <sup>7</sup> GpppG	60.0 ± 3.0	
m <sup>7</sup> GpppXG D1	<b>1a</b>	41.4 ± 0.4
m <sup>7</sup> GpppXG D2	<b>1b</b>	64.3 ± 0.6
m <sup>7</sup> GpppXpG D1	<b>2a</b>	52.5 ± 0.5
m <sup>7</sup> GpppXpG D2	<b>2b</b>	54.1 ± 0.5
m <sup>7</sup> GpXppG D1	<b>3a</b>	60.1 ± 0.6
m <sup>7</sup> GpXppG D2	<b>3b</b>	44.2 ± 0.4

<sup>a</sup>The extent of stacking was determined in 0.1 M phosphate buffer, pH 5.2, at 20°C from the fluorescence intensity of 7-methylguanosine as described in the Materials and Methods section. The data represent the mean ± SD.

tial hydrolysis during reaction work-up and purification on DEAE Sephadex ion-exchange resin. A pilot coupling reaction between **7** and **8** in the presence of a ZnCl<sub>2</sub> excess, monitored using RP HPLC, revealed formation of the desired product (**1**) but also a significant level of P-BH<sub>3</sub>-bond cleavage resulting in the conversion of **7** to guanosine 5'-(H-phosphonate). Therefore, we tested other metal ions and conditions to optimize the reaction (Supplementary Table S1). The reaction was most efficient in the presence of 8 equiv. of MgCl<sub>2</sub> in DMF, although its progress was rather slow because the final conversion was achieved only after 7 days. It could be accelerated by addition of up to 10% of water to DMF, which probably increased solubility of the magnesium chloride. However, this also caused hydrolysis of **7** to guanosine and boranophosphate, which diminished the overall yield (for the same reason, coupling in fully aqueous media gave poor results; Supplementary Table S1). Synthesis of **1** could be, however, shortened to 10 h without compromising the yield by using microwave irradiation (**39**). Under optimized conditions, the synthesis was completed with a 62% isolated yield. The formation of a new pyrophosphate bond resulted in the new stereogenic phos-

phorus center and the presence of two P-diastereomers of the desired cap analog. These diastereomers were separated by RP HPLC and designated D1 (**1a**) and D2 (**1b**), based on their elution order (Figure 2C). They were analyzed as diastereomerically pure forms in the subsequent experiments. Using analogous conditions for the reaction of **7** with **9**, two diastereomers of the ARCA modified at the α-position (**5**) were synthesized with a 60% yield.

To synthesize cap analogs modified at the γ-position (**3**), we initially tried a similar strategy. Hence, 7-methylguanosine monoboranophosphate (**10**) was synthesized from **7** by treatment with methyl iodide in DMSO. A level of cleavage up to 10% of the monoboranophosphate to H-phosphonate and oxidation to a monophosphate (m<sup>7</sup>GMP) were observed under these conditions. Despite these side-reactions and hydrolysis during reaction work-up, the product (**10**) was isolated with a 52% yield. Next, **10** was subjected to coupling with **11** under conditions analogous to those for **1**. However, formation of the desired product was not observed, even after a long reaction period and under variously altered conditions. Only formation of nucleotides derived by hydrolysis- and self-coupling (GDP and Gp<sub>4</sub>G) was observed, and compound **10** was gradually hydrolyzed to 7-methylguanosine and inorganic boranophosphate. Therefore, **3** was synthesized by a different route in which the dinucleotide was formed after formation of 7-methylguanosine α-boranodiphosphate (**13**) and guanosine 5'-phosphorimidazolide (**14**). Guanosine α-boranodiphosphate (**12**) was first synthesized from **7** and (2-cyanoethyl)phosphorimidazolide lithium salt (**39**) and then methylated at the N<sup>7</sup> position using methyl iodide in DMSO to afford **13**. In contrast to the synthesis of **10**, no side-processes associated with boranophosphate cleavage to H-phosphonate, hydrolysis or oxidation were observed upon treatment with methyl iodide. Consequently, compound **13** was isolated in a 70% yield. The MgCl<sub>2</sub>-mediated coupling of **13** with **14** was also efficient with only a few hours required for completion.



**Table 4.** Susceptibility of BH<sub>3</sub>-analogs to the decapping scavenger (DcpS) under high enzyme concentrations (*Assay II*)

No.	Reaction time (min)	Percent of cleavage, $x$ (%) <sup>a</sup>			
		hDcpS		CeDcpS	
		10	90	10	90
	m <sup>7</sup> GpppG	100	100	100	100
<b>2a</b>	m <sup>7</sup> GppBH <sub>3</sub> pG D1	3	12	100	100
<b>2b</b>	m <sup>7</sup> GppBH <sub>3</sub> pG D2	3	19	90	100
<b>3a</b>	m <sup>7</sup> GpBH <sub>3</sub> ppG D1	2	11	1	6
<b>3b</b>	m <sup>7</sup> GpBH <sub>3</sub> ppG D2	27	98	50	97
<b>4</b>	m <sup>7</sup> GppBH <sub>3</sub> pm <sup>7</sup> G	2	3	20	60
	m <sup>7</sup> GpsppG D1	1	4	15	74
	m <sup>7</sup> GpsppG D2	0	0	0	0
	m <sup>7</sup> GppsppG D1	100	100	100	100

<sup>a</sup>Reactions contained the DcpS enzyme at 200 nM and cap analogs at 15 μM in 50 mM Tris-HCl buffer, containing 200 mM KCl, 0.5 mM EDTA and 1 mM DTT (final pH 7.6), at 20°C. Samples collected at various time points were pretreated as described in the Materials and Methods section and analyzed using RP HPLC with absorbance detection at 260 nm and fluorescence detection at 337 nm (excitation at 280 nm). The percentage of hydrolyzed cap ( $x$ ) was calculated according to the equation  $x = (A_{P1} + A_{P2}) / (A_{P1} + A_{P2} + 1.1 \cdot A_S) \cdot 100\%$ , where  $A_{P1}$ ,  $A_{P2}$  and  $A_S$  are areas of the peaks corresponding to the GDP-like or GDP-derived product, m<sup>7</sup>GMP-like product and substrate, respectively.  $A_S$  is multiplied by factor 1.1 to compensate for the extinction coefficient change upon hydrolysis. Standard deviation of  $x$  is less than 5%.

The assay was performed using DcpS from humans and from *C. elegans*. High enzyme concentration was used to select analogs suitable for the fluorescence-based binding assay. The reactions were monitored by HPLC as described in the Materials and Methods section, *Assay II*. The results were compared to the unmodified parent cap (m<sup>7</sup>GpppG) and selected S-analogs. Compounds **1a** and **1b** were not included in this assay since even under lower enzyme concentrations they were hydrolyzed by DcpS with rates comparable to m<sup>7</sup>GpppG.

**Table 5.** Equilibrium association constants ( $K_{AS}$ ) for the complexes of mouse eIF4E(28–217) with dinucleotide cap analogs substituted in the phosphate chain with BH<sub>3</sub> or S

No.	Compound	$K_{AS}$ (μM <sup>-1</sup> ) <sup>a</sup>
	m <sup>7</sup> GpppG <sup>b</sup>	12.5 ± 0.3
	m <sub>2</sub> <sup>7,2'-O</sup> GpppG <sup>c</sup>	10.8 ± 0.3
	m <sup>7</sup> Gpppm <sup>7</sup> G <sup>b</sup>	5.0 ± 0.2
<b>1a</b>	m <sup>7</sup> GpppBH <sub>3</sub> G D1	14.5 ± 0.2
<b>1b</b>	m <sup>7</sup> GpppBH <sub>3</sub> G D2	14.4 ± 0.6
<b>2a</b>	m <sup>7</sup> GppBH <sub>3</sub> pG D1	44.0 ± 1.8
<b>2b</b>	m <sup>7</sup> GppBH <sub>3</sub> pG D2	13.0 ± 0.2
<b>3a</b>	m <sup>7</sup> GpBH <sub>3</sub> ppG D1	9.6 ± 0.3
<b>3b</b>	m <sup>7</sup> GpBH <sub>3</sub> ppG D2	17.3 ± 0.2
<b>4</b>	m <sup>7</sup> GppBH <sub>3</sub> pm <sup>7</sup> G <sup>d</sup>	11.1 ± 0.2
<b>5a</b>	m <sub>2</sub> <sup>7,2'-O</sup> GpppBH <sub>3</sub> G D1	15.3 ± 0.2
<b>5b</b>	m <sub>2</sub> <sup>7,2'-O</sup> GpppBH <sub>3</sub> G D2	16.0 ± 0.4
<b>6a</b>	m <sub>2</sub> <sup>7,2'-O</sup> GppBH <sub>3</sub> pG D1 <sup>d</sup>	39.4 ± 1.2
<b>6b</b>	m <sub>2</sub> <sup>7,2'-O</sup> GppBH <sub>3</sub> pG D2 <sup>d</sup>	13.2 ± 0.2
	m <sup>7</sup> GpsppG D1 <sup>c</sup>	30.8 ± 0.5
	m <sup>7</sup> GpsppG D2 <sup>c</sup>	10.0 ± 0.2
	m <sup>7</sup> GppsppG D1 <sup>c</sup>	45.0 ± 1.1
	m <sup>7</sup> GppsppG D2 <sup>c</sup>	23.0 ± 0.4

<sup>a</sup>50 mM HEPES/KOH (pH 7.2), 100 mM KCl, 0.5 mM EDTA and 1 mM DTT at 20°C.

<sup>b</sup>Data from (34).

<sup>c</sup>Data from (7).

<sup>d</sup>Data from (35).

The  $K_{AS}$  values were determined by time-synchronized fluorescence quenching titration as described in the Materials and Methods section.

Finally, we attempted the synthesis of cap dinucleotides modified at the β-position of the triphosphate bridge (**2**, **4** and **6**). First, a symmetrical dinucleotide, diguanosine 5'-(2-boranotriphosphate) (**15**) was obtained by coupling of GMP-Im (**14**) excess with boranomonomophosphate. Then, **15** was N<sup>7</sup>-methylated with methyl iodide in DMSO. The formation of two products was observed, a single-methylated

cap analog **2** and double-methylated cap analog **4** (Supplementary Figure S1). The reaction required careful monitoring by HPLC to avoid pyrophosphate cleavage side-reactions. The double methylated (two-headed) cap analog **4** was expected to be a useful reagent for synthetic mRNA preparation as due to its pseudo-symmetry it has no P-diastereomers and due to the presence of two m<sup>7</sup>G moieties it cannot be incorporated into mRNA in the 'reverse' orientation. Therefore, **4** was synthesized also by direct coupling of 7-methylguanosine 5'-phosphorimidazolide (**16**) with boranophosphate, which resulted in a 57% yield. The synthesis of ARCA modified at the β-position (**6**) was attempted using a two-step route proceeding through a nucleoside 2-boranodiphosphate intermediate. Unfortunately, both guanosine 2-boranodiphosphate and N<sup>7</sup>,2'-O-dimethylguanosine 2-boranodiphosphate (synthesized by coupling of the corresponding nucleoside phosphorimidazolide with excess boranophosphate) intermediates were not sufficiently stable to be isolated (quickly hydrolyzed to nucleoside monophosphates and boranophosphate anion). Therefore, cap analog **6** was synthesized by a one-pot approach in which the unstable intermediate was subjected to coupling with **14** without isolation. Due to formation of by-products in the self-coupling reaction, the desired compound **6** was isolated with a 41% yield.

To broaden the scope of our chemical approach, we attempted the synthesis of other boranophosphate-modified nucleotides (Figure 6). To synthesize diadenosine (1,3-diboranophosphate) (**21**), an analog of Ap<sub>3</sub>A bearing two boranophosphate groups (at the α- and γ- positions) (Scheme 4A), adenosine 5'-boranophosphate (**18**) was first obtained from adenosine H-phosphonate similarly to **7** and then converted into adenosine α-boranodiphosphate (**19**) by coupling with (2-cyanoethyl)phosphorimidazolide (**39**). Then, **19** was converted into its P-imidazolide derivative (**20**), showing that α-boranodiphosphates (in contrast to

**Table 6.** Binding affinities of the unhydrolyzable BH<sub>3</sub>-analogs for the human and *C. elegans* DcpS

No.	Compound	K <sub>AS</sub> for hDcpS <sup>a</sup> (μM <sup>-1</sup> )	K <sub>AS</sub> for CeDcpS <sup>a</sup> (μM <sup>-1</sup> )
	m <sup>7</sup> GpppG	n.d. (hydrolyzed)	n.d. (hydrolyzed)
	m <sup>7</sup> GDP	114 ± 8 <sup>b</sup>	97 ± 12 <sup>c</sup>
<b>2a</b>	m <sup>7</sup> GppBH <sub>3</sub> pG D1	63.2 ± 3.1	n.d. (hydrolyzed)
<b>2b</b>	m <sup>7</sup> GppBH <sub>3</sub> pG D2	40.7 ± 2.6	n.d. (hydrolyzed)
<b>3a</b>	m <sup>7</sup> GppBH <sub>3</sub> ppG D1	77.4 ± 5.4	40.0 ± 1.9
<b>3b</b>	m <sup>7</sup> GppBH <sub>3</sub> ppG D2	n.d. (hydrolyzed)	n.d. (hydrolyzed)
<b>4</b>	m <sup>7</sup> GppBH <sub>3</sub> pm <sup>7</sup> G	67.1 ± 8.5	n.d. (hydrolyzed)
<b>6a</b>	m <sub>2</sub> <sup>7,2'-O</sup> GppBH <sub>3</sub> pG D1	64.6 ± 6.0	n.d. (hydrolyzed)
<b>6b</b>	m <sub>2</sub> <sup>7,2'-O</sup> GppBH <sub>3</sub> pG D2	55.3 ± 6.4	n.d. (hydrolyzed)
	m <sup>7</sup> GpNHppG	218 ± 24 <sup>d</sup>	66 ± 9 <sup>c</sup>
	m <sup>7</sup> GpCH <sub>2</sub> ppG	234 ± 14 <sup>e</sup>	8.6 ± 0.4 <sup>c</sup>
	m <sup>7</sup> GpSppG D1	146 ± 6 <sup>b</sup>	n.d. (hydrolyzed)
	m <sup>7</sup> GpSppG D2	121 ± 10 <sup>b</sup>	69 ± 6 <sup>c</sup>

<sup>a</sup>Determined in 50 mM Tris HCl, 200 mM KCl, 0.5 mM EDTA and 1 mM DTT (final pH 7.6) at 20.0 ± 0.3°C.

<sup>b</sup>Data from (36).

<sup>c</sup>Data from (31,37).

<sup>d</sup>Data from (9).

<sup>e</sup>Data from (6).

n.d.: the K<sub>AS</sub> value could not be determined because the analog was not sufficiently stable in the presence of enzyme.

The equilibrium association constants for cap–DcpS complexes were determined by time-synchronized fluorescence quenching titration as described in the Materials and Methods section. Corresponding data for selected previously reported DcpS-resistant cap analogs are included for comparison.

**Table 7.** Inhibition of translation of luciferase mRNA by BH<sub>3</sub>-analogs in RRLs

	Setup A (no pre-incubation) IC <sub>50</sub> (μM) <sup>a</sup>	Setup B (cap pre-incubated) IC <sub>50</sub> (μM) <sup>a</sup>
m <sup>7</sup> GpppG	8.30 ± 0.47 (n = 10)	27.1 ± 1.9 (n = 8)
m <sup>7</sup> GpppBH <sub>3</sub> G D1 ( <b>1a</b> )	2.94 ± 0.28 (n = 2)	8.35 ± 1.76 (n = 2)
m <sup>7</sup> GpppBH <sub>3</sub> G D2 ( <b>1b</b> )	2.83 ± 0.16 (n = 2)	14.90 ± 0.56 (n = 2)
m <sup>7</sup> GppBH <sub>3</sub> pG D1 ( <b>2a</b> )	1.27 ± 0.07 (n = 7)	1.16 ± 0.10 (n = 6)
m <sup>7</sup> GppBH <sub>3</sub> pG D2 ( <b>2b</b> )	4.09 ± 0.33 (n = 3)	3.15 ± 0.58 (n = 3)
m <sup>7</sup> GppBH <sub>3</sub> ppG D1 ( <b>3a</b> )	4.31 ± 0.71 (n = 4)	3.66 ± 0.28 (n = 2)
m <sup>7</sup> GppBH <sub>3</sub> ppG D2 ( <b>3b</b> )	3.26 ± 0.28 (n = 4)	5.50 ± 0.50 (n = 2)
m <sup>7</sup> GppBH <sub>3</sub> pm <sup>7</sup> G ( <b>4</b> )	2.77 ± 0.10 (n = 3)	2.76 ± 0.14 (n = 4)

<sup>a</sup>Cap analog concentration (in μM) at which cap-dependent translation in RRL is reduced by 50%. Presented IC<sub>50</sub> values are means of 2–10 experiments and normalized to the IC<sub>50</sub> value of m<sup>7</sup>GpppG = 8.3 (as described in (22)).

In experimental setup A, the cap analog and luciferase mRNA were added to RRL at the same time point. In setup B the cap analog was preincubated in RRL for 60 min prior to addition of mRNA (Supplementary Figure S6). A relative loss of inhibitory properties in setup B indicates for susceptibility to degradation in RRL.

**Table 8.** The influence of different mRNA cap analogs on luciferase expression in hiDCs

5'-cap analog	Translational efficiency <sup>a</sup>	Time of max. (h)	Total protein expression <sup>a</sup>
m <sub>2</sub> <sup>7,3'-O</sup> GpppG	1.00 ± 0.00	11.45 ± 0.07	1.00 ± 0.01
m <sup>7</sup> GpppG	0.63 ± 0.02	8.95 ± 0.07	0.41 ± 0.02
m <sub>2</sub> <sup>7,2'-O</sup> GppspG D1	1.29 ± 0.16	15.55 ± 0.21	2.19 ± 0.22
m <sub>2</sub> <sup>7,2'-O</sup> GppspG D2	1.78 ± 0.33	10.75 ± 0.21	1.60 ± 0.25
m <sup>7</sup> GppBH <sub>3</sub> pm <sup>7</sup> G ( <b>4</b> )	0.94 ± 0.04	10.80 ± 0.00	0.83 ± 0.03
m <sub>2</sub> <sup>7,2'-O</sup> GppBH <sub>3</sub> pG D1 ( <b>6a</b> )	1.11 ± 0.15	17.45 ± 0.21	2.25 ± 0.35
m <sub>2</sub> <sup>7,2'-O</sup> GppBH <sub>3</sub> pG D2 ( <b>6b</b> )	1.37 ± 0.03	12.65 ± 0.07	1.66 ± 0.02

<sup>a</sup>Values are given relative to results for ARCA-capped mRNA.

Experimental data depicted in Figure 8 were fitted using spline interpolation which produces values of translational efficiency (maximal slope), functional RNA stability (time point of maximal protein expression) and the total protein expression (integral of the curve), as induced by the differentially 5'-capped mRNAs (listed are averaged values from duplicate measurements ± SD).

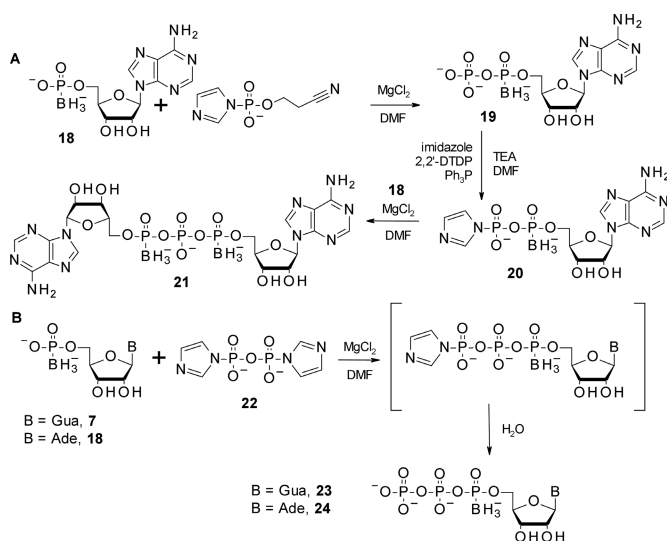


**Figure 6.** Synthesis of guanosine and adenosine  $\alpha$ -boranotriphosphates and diadenosine 1,3-diboranotriphosphate by means of phosphorimidazole chemistry.

$\alpha$ -thiodiphosphates) may be efficiently converted to  $P^2$ -electrophilic species. As a result of coupling **20** with **18** in the presence of  $\text{MgCl}_2$  compound **21** was isolated with a 70% yield after DEAE Sephadex chromatography as a mixture of three diastereomers (D1- $S_P$ ,  $S_P$ , D2- $S_P$ ,  $R_P$  and D3- $R_P$ ,  $R_P$ ), which could be partially resolved using RP HPLC (Supplementary Figure S2). We also tested whether nucleoside 5'-boranophosphates can be used as starting materials for the synthesis of nucleoside  $\alpha$ -boranotriphosphates by coupling with pyrophosphate P1,P2-diimidazolyl derivative (**22**) (Figure 6) (40). If a 4-fold excess of **22** was used in coupling with **7** or **18** almost exclusive formation of nucleoside guanosine (**23**) and adenosine  $\alpha$ -boranotriphosphates (**24**), respectively, was observed. Small amounts of nucleoside 5'- $\alpha$ -boranopentaphosphates were also formed under these conditions and their fraction could be elevated by increasing the excess of **22**. After aqueous work-up and ion-exchange purification, **23** and **24** were isolated with a 44% and a 52% yield, respectively.

**Spectroscopic and stereochemical characterization.** All the synthesized analogs, after being resolved into pure  $P$ -diastereomers using RP HPLC, were characterized by mass spectrometry, NMR, and UV-VIS absorption and emission spectroscopy to confirm their structures and homogeneities and to determine the extent to which the presence of the boranophosphate moiety influences basic physicochemical properties of the cap. Since the cap  $\text{BH}_3$ -analogs and related nucleotides were diastereomerically pure, we attempted assignment of stereogenic  $P$ -center configurations by correlation with structurally related compounds (Table 2) (41,42). The most straightforward was the analysis of cap analogs **1** and **4** modified at the  $\alpha$ -position because they could be correlated with  $\text{GDP}\alpha\text{BH}_3$  diastereomers, for which absolute  $P$ -stereochemistry had been determined previously (41). The reaction of **8** with  $\text{GDP}\alpha\text{BH}_3$ , D1 ( $R_P$ -isomer, **12a**) produced the faster eluting diastereomer of  $m^7\text{GpppBH}_3\text{G}$ , D1

(**1a**), indicating simply that **1a** has the same ( $R_P$ ) configuration as **12a**. Similarly, the configuration was assigned for the diastereomers of  $m^7,2'-O\text{GpppBH}_3\text{G}$  (**5**). To determine the absolute configurations of  $m^7\text{GpBH}_3\text{ppG}$   $P$ -diastereomers (**3a** and **3b**), we first correlated the stereochemistry of  $\text{GDP}\alpha\text{BH}_3$  (**12**) with  $m^7\text{GDP}\alpha\text{BH}_3$  (**13**). HPLC monitoring of the methylation reaction of an unequimolar diastereomeric mixture of **12a** and **12b** revealed that the order of elution of the methylated products, **13a** and **13b**, from an RP HPLC column was reversed compared to the unmethylated substrates (Supplementary Figure S3). In a separate experiment, we confirmed that  $\text{GDP}\alpha\text{BH}_3$ , D1 (**12a**) produces exclusively  $m^7\text{GDP}\alpha\text{BH}_3$ , D2 (**13b**) upon treatment with methyl iodide, i.e. both compounds have the same ( $R_P$ ) absolute configuration. When the diastereomers of **13** were coupled to **14** to produce dinucleotide cap analog **3**, the order of elution was preserved, meaning the slower-eluting  $m^7\text{GpBH}_3\text{ppG}$ , D1 (**3b**) has the  $R_P$  configuration. The absolute configuration of cap analogs modified at the  $\beta$ -position remains to be determined.

Subsequently, we investigated basic conformational properties of the  $\text{BH}_3$ -analogs. In dinucleotides such as  $m^7\text{GpppG}$ , the positively charged 7-methylguanine has a strong tendency to form cation- $\pi$  complexes with the second nucleobase, in a base-stacking interaction (**30**). Hence, cap analogs in solution are in a dynamic equilibrium between stacked and unstacked conformations. In the stacked conformation, the intrinsic fluorescence of 7-methylguanosine is partially quenched. Hence, the proportion of the two forms can be calculated from the relative fluorescence intensity. For  $\text{BH}_3$ -analogs **1a–3b**, the values for % stacking ranged from 41% to 65% compared to 61% for  $m^7\text{GpppG}$  (Table 3), being in the typical range of other cap dinucleotides and being generally similar to the values of corresponding  $S$ -analogs (27). For dinucleotides with the modified-phosphate group adjacent to a nucleoside moiety (either G or  $m^7\text{G}$ ), the analogs bearing an O to  $\text{BH}_3$  or O to S substitution at the *pro-S\_P*-position (i.e.  $R_P$   $\text{BH}_3$ -analogs and  $S_P$   $S$ -analogs) had an up to 30% lower fraction of the stacked form than corresponding *pro-R\_P*-substituted analogs, or unmodified analog. More detailed information on the conformation of nucleoside moieties, e.g. the ribose puckering, can be derived from  $^1\text{H}$  NMR data. The  $S$  and  $N$  conformer populations for both guanosine and 7-methylguanosine in cap analogs **1–6** and in other synthesized boranophosphate-containing nucleotides are in the range of typical values (Supplementary Table S2).

$^1\text{H}$  NMR chemical shifts have also been shown to be useful for predicting the  $S_P/R_P$  configurations around phosphorus centers (41,42). It has been reported that the  $\delta$  ppm values for H8 protons of purine nucleotides such as  $\text{NTP}\alpha\text{X}$  and  $\text{NDP}\alpha\text{X}$  ( $N = \text{A or G}$ ,  $X = \text{S or BH}_3$ ) are particularly useful for assigning the absolute configuration to stereogenic  $\alpha$ -phosphorus atoms (41,42). According to the previous observations, the diastereomer migrating faster in an RP HPLC column (D1) is the *pro-S\_P* oxygen substituted isomer (i.e. with  $\alpha$ -S  $S_P$  or  $\alpha$ - $\text{BH}_3$   $R_P$  configuration) and has less shielded H8 protons (i.e. with a higher  $\delta$ -ppm value compared to D2). We compared the  $\delta$ -ppm  $^1\text{H}$  NMR for the diastereomeric pairs of all synthesized mono- and dinucleotides modified with boranophosphate at a position ad-

adjacent to the nucleoside (e.g. guanosine for compounds **1**, **4**, **12** and 7-methylguanosine for compounds **3**, **13**; and others) and some of their phosphorothioate counterparts (Supplementary Table S2). The great majority of these compounds followed the rule reported previously in the literature, i.e. for BH<sub>3</sub>-analogs the diastereomer of *R<sub>P</sub>* configuration (eluted as ‘faster’, i.e. D1) had a more deshielded H8 proton (just like S-analogs with *S<sub>P</sub>* configuration). Differences of +0.1 to +0.5-ppm  $\Delta\delta_{\text{H8}}$  between *S<sub>P</sub>* and *R<sub>P</sub>* isomers were observed, except in two examples. For compound **13** (m<sup>7</sup>GDP $\alpha$ BH<sub>3</sub>), neither the order of elution nor the H8 chemical shift followed this rule (D1 isomer = *S<sub>P</sub>*;  $\Delta\delta_{\text{H8}} = -0.09$  ppm; Table 3). In cap analog **3** (m<sup>7</sup>Gp<sub>BH3</sub>ppG), the order of HPLC elution was reversed, but the H8 proton shift correlated with the absolute configuration as previously reported with  $\Delta\delta_{\text{H8}}$  of +0.10 ppm. Therefore, the absolute configuration assignment for those compounds based just on RP HPLC mobility and <sup>1</sup>H NMR data could be incorrect. However, for all tested BH<sub>3</sub>-analogs even greater differences than those for H8 protons in the *S<sub>P</sub>* and *R<sub>P</sub>* isomers were observed for the corresponding H3' protons with  $\Delta\delta_{\text{H3'}}$  always positive (Table 3). This effect appeared to be independent of the ribose conformation because it was observed both for standard purine nucleotides (C2' endo prevalent) and for m<sup>7</sup>G nucleotides (C3' endo prevalent) (Supplementary Table S1 and Supplementary Figure S4). Therefore, the H3' proton shift may be more reliable for the analysis of P-center absolute configurations in boranophosphate nucleotide analogs. The same rule could be applied to the phosphorothioate nucleotides, but the  $\Delta\delta_{\text{H3'}}$  differences were smaller, and for some nucleotides (but not m<sup>7</sup>G ones), the H3' signals of D1 and D2 did not differ. Molecular dynamics simulations for m<sup>7</sup>GDP $\alpha$ X and GDP $\alpha$ X, where X is either BH<sub>3</sub> or S, confirmed that the average X-H3' distances were different for *S<sub>P</sub>* and *R<sub>P</sub>* stereoisomers (Table 3).

## BIOLOGICAL PROPERTIES

### Susceptibility to degradation by DcpS

DcpS belongs to the HIT protein family of pyrophosphatases, (43) which contain a conserved Histidine Triad (HIT) motif, His-X-His-X-His. The enzyme cleaves m<sup>7</sup>GpppN dinucleotides and short capped mRNA oligonucleotides, but not long capped mRNAs (17). Human DcpS (hDcpS) cleaves dinucleotides such as m<sup>7</sup>GpppG exclusively between the  $\gamma$ - and  $\beta$ -phosphates to release m<sup>7</sup>GMP and GDP, performing its catalysis via the attack of His 277 (middle histidine of the HIT motif) at the cap's  $\gamma$ -phosphate. Consequently, replacing the  $\beta$ - $\gamma$  bridging oxygen by a CH<sub>2</sub> or NH group or one of the non-bridging  $\gamma$ -oxygens by sulfur produces hDcpS-resistant cap analogs (14). In contrast, corresponding modifications at the bridging  $\alpha/\beta$ -position or non-bridging  $\alpha$ - and  $\beta$ -positions do not confer resistance. To evaluate the influence of boranophosphate substitutions on the susceptibility to DcpS, we studied the DcpS-mediated hydrolysis of BH<sub>3</sub>-analogs by an HPLC-based assay, under experimental conditions enabling comparison of our data with results on previously reported cap analogs (a 40- $\mu$ M cap analog and a 100-nM enzyme; the Materials and Methods section, Assay 1). In addition to hDcpS, we studied its *C. elegans* homolog

(CeDcpS), (44) for which less data are available in the literature (31,37,45). Under the conditions tested, the reference cap, m<sup>7</sup>GpppG, was almost completely hydrolyzed within 15–30 min. Shown in Figure 7 are representative HPLC profiles from the assay, and the results obtained for BH<sub>3</sub>-analogs with hDcpS and CeDcpS are summarized in Supplementary Table S3. All BH<sub>3</sub>-analogs that under the same conditions were degraded by less than 10% within 2 h, compared to the control with no enzyme, were preliminarily assumed to be DcpS-resistant. The BH<sub>3</sub>-analogs varied in their susceptibility to DcpS from being comparable with m<sup>7</sup>GpppG to being resistant (Figure 7). In some cases, the susceptibility of particular analogs differed between hDcpS and CeDcpS. For hDcpS, not only  $\gamma$ -modified (**3a** and **3b**), but also  $\beta$ -modified BH<sub>3</sub>-analogs (**2a**, **2b** and **4**) turned out to be unhydrolyzable, which was unexpected because the corresponding  $\beta$ -phosphorothioates are good substrates for hDcpS (7). In contrast, for CeDcpS, only the analogs modified at the  $\gamma$ -position were resistant to degradation by CeDcpS, whereas the other BH<sub>3</sub>-analogs were susceptible, however, the  $\beta$ -modified ones were hydrolyzed substantially slower than m<sup>7</sup>GpppG. To verify the resistance under more rigorous conditions of binding studies, we performed another assay under more rigorous conditions. In this experiment, 200-nM enzyme and 15- $\mu$ M cap analog were used to emulate the final stages of a typical binding experiment (see the next subsection) (the Materials and Methods section, Assay 2). Some of the corresponding S-analogs were also included for comparison. The results of this assay (Table 4) confirmed the unusual regioselectivity of hDcpS, as all  $\beta$ -BH<sub>3</sub> analogs (**2a**, **2b** and **4**) were resistant to DcpS even under those more rigorous conditions. The two-headed analog **4** was the least susceptible boranophosphate cap analog in this study, with resistance comparable only to m<sup>7</sup>Gp<sub>S</sub>ppG D2. As expected, CeDcpS hydrolyzed all  $\beta$ -borano cap analogs under high enzyme concentration (Table 4). Interestingly, experiments on the  $\gamma$ -modified BH<sub>3</sub>-analogs revealed stereoselectivity of hydrolysis catalyzed by DcpS enzymes, regardless of their origin. Both human and *C. elegans* DcpS enzymes hydrolyze the D2 isomer of the  $\gamma$ -modified BH<sub>3</sub>-analog (**3b**; *R<sub>P</sub>* configuration), unlike its D1 counterpart (**3a**; *S<sub>P</sub>* configuration); 98% and 11% of hydrolysis after 90 min, respectively. The products of hydrolysis were m<sup>7</sup>GMPBH<sub>3</sub> and GDP, meaning that the boranophosphate group was preserved during the reaction. No side-processes such as P-B-bond cleavage were detected, suggesting that the mechanism of hydrolysis remains essentially the same as for m<sup>7</sup>GpppG. For S-analogs, stereoselectivity toward the analog with the same spatial configuration was observed (i.e. m<sup>7</sup>Gp<sub>S</sub>ppG D1, *S<sub>P</sub>*). However, the difference was far less pronounced, as both stereoisomers were hydrolyzed not more than 10% after 180 min.

### Binding affinities for DcpS and eIF4E

To determine the binding affinity of BH<sub>3</sub>-analogs for DcpS and eIF4E, we employed time-synchronized fluorescence-quenching titration method (32,46). For DcpS, the binding affinity could be determined only for analogs that were resistant to hydrolysis at a high enzyme concentration present

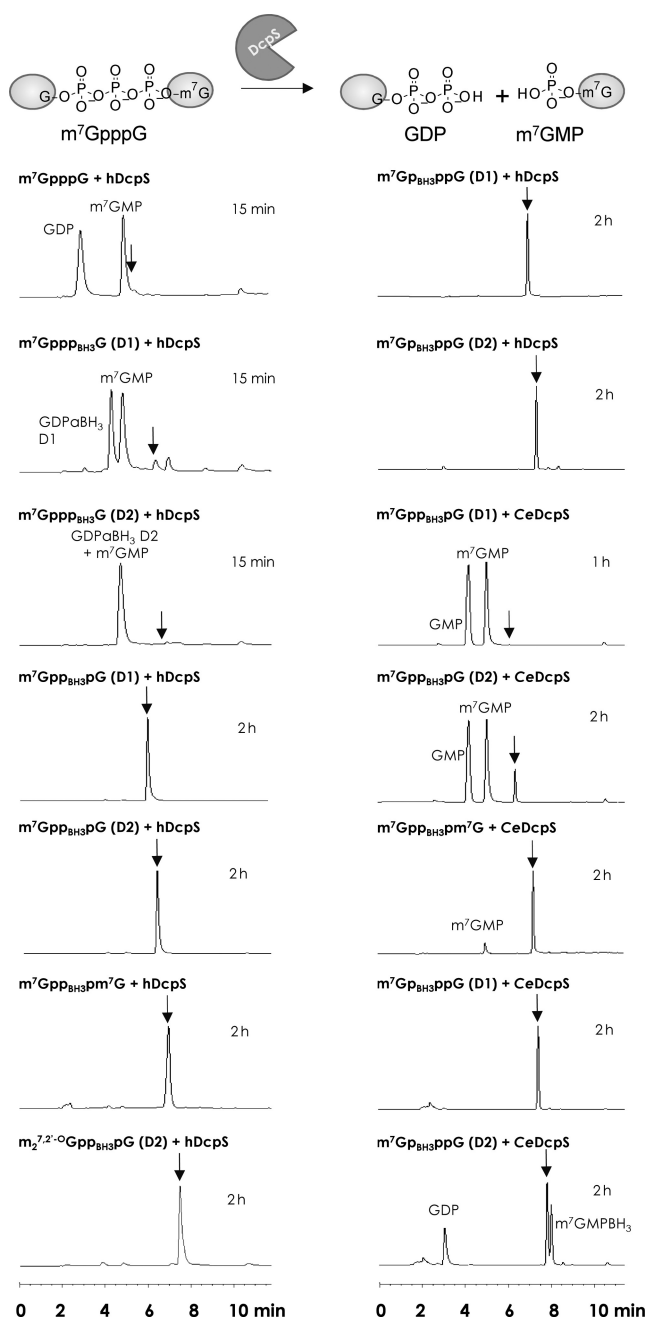


**Figure 7.** Representative HPLC profiles from the DcpS-susceptibility assay at lower enzyme concentration (*Assay I*).  $BH_3$ -analogs were incubated at  $40 \mu M$  with  $100$ -nM human or *C. elegans* DcpS and aliquots taken at different time points were analyzed by RP HPLC at  $260$  nm as described in the Materials and Methods section. The analogs that were hydrolyzed in less than  $10\%$  within  $2$  h were assumed to be resistant to DcpS (see Supplementary Table S2). The black arrow in each panel indicates the retention time at which the reaction substrate is eluted. The initial degradation products of  $\beta$ -modified analogs are  $m^7GMP$  and guanosine  $\beta$ -boranodiphosphate ( $GDP\beta BH_3$ ); however, the latter is chemically labile and rapidly hydrolyses to GMP during high-temperature deactivation of the enzyme (data not shown).

in the titration experiment, as described in the previous subsection. Representative titration curves are shown in Supplementary Figure S5, whereas the mean  $K_{AS}$  values for the eIF4E-cap and DcpS-cap complexes obtained from replicate experiments are summarized in Tables 5 and 6, respectively, together with the same data for selected previously reported cap analogs (9,34–37). These data indicate that the boranophosphate moiety, similarly to phosphorothioate moiety, does not destabilize the eIF4E-cap complex. The  $K_{AS}$  values for the  $BH_3$ -caps were either equal to or higher than  $K_{AS}$  for the eIF4E- $m^7GpppG$  complex and were dependent on the position and absolute configuration of the stereogenic phosphorus center. For S-analogs, the D1 isomers have generally higher affinity to eIF4E than their D2 counterparts (7). This tendency was also observed in  $BH_3$ -analogs, with exception of the  $m^7Gp_{BH_3}ppG$  (3), for which D2 has 2-fold higher  $K_{AS}$  than does D1. This result is fully consistent with the finding that the  $BH_3$ - $\gamma$ -D2 isomer has the spatial configuration same as S- $\gamma$ -D1. On the other hand, the boranophosphate moiety had a rather destabilizing effect on the hDcpS-cap complexes (Table 6). A similar destabilizing effect was previously observed for S-analogs, but the  $BH_3$ -analogs had hDcpS- $K_{AS}$  values up to 2-fold lower. Hence, when compared to  $m^7GpppG$ , the  $BH_3$ -analogs may be considered as tight binders for eIF4E and rather poor binders for DcpS.

### Inhibition of cap-dependent translation

The potential of  $BH_3$ -analogs as inhibitors of protein translation was tested *in vitro* in RRLs, where capped reporter luciferase mRNA was translated in the presence of various concentrations of an analyzed cap analog (Table 7 and Supplementary Figures S5 and S6). The  $IC_{50}$  values, resulting from fitting the experimental data to a theoretical curve as described in the Materials and Methods section, revealed that all tested  $BH_3$ -analogs were generally better inhibitors of translation in this system than  $m^7GpppG$ . Under the standard experimental conditions (experimental setup A; Table 7, column A), in which the tested cap analog was added to the RRL at the same time point as mRNA (Supplementary Figure S6), the  $IC_{50}$  values for  $BH_3$ -analogs ranged from  $1.3$  to  $4.3 \mu M$ , compared to  $8.3 \mu M$  for  $m^7GpppG$ . To evaluate the stability of cap analogs in the cell lysate conditions, another type of experiment was performed (experimental setup B; Table 7, column B) in which a cap analog was added to the RRL  $60$  min prior to the addition of mRNA and translation start. In this setup, some of the compounds lost their inhibitory properties to a significant extent. Only the compounds that were determined to be DcpS-resistant through the HPLC-based assay remained potent inhibitors after pre-incubation in RRL (Supplementary Figure S6 and Table 7). There was no correlation between affinity for eIF4E and  $IC_{50}$  values, especially in the second experimental setup.  $m^7Gpp_{BH_3}pG$  D1 (2a) and  $m^7Gpp_{BH_3}pm^7G$  (4) were the two most stable and potent inhibitors, being 6.3- and 2.9-fold more potent than  $m^7GpppG$ , respectively, in the experiment without cap pre-incubation. After incubation in RRL the differences became even more pronounced (the corresponding  $IC_{50}$  val-

ues were, respectively, 23- and 10-fold lower than the  $IC_{50}$  of  $m^7GpppG$ ).

### Translational efficiency in dendritic cells

Modified cap analogs are interesting not only as small molecules selectively targeting cap-related proteins. They have also been found to strongly influence the characteristics of mRNA once introduced into their 5' end by *in vitro* transcription (16,47). RNAs carrying boranophosphate cap structures **4**, **6a** and **6b** have been tested in a related study in HeLa cells (35,48). However, differences in the effects of cap modifications in different cell types have been described (12). Therefore, we tested RNAs capped with boranophosphate caps in hiDCs, the major antigen-presenting cells of the immune system. These cells are of interest in terms of RNA-based immunotherapeutic approaches against cancer (49). Importantly, an increase in the efficacy of an mRNA-induced immune response against an RNA-encoded antigen by means of modified cap dinucleotides for respective 5'-capping has been described (12).

We decided to analyze the effects of ARCA-type analogs modified with a boranophosphate group at the  $\beta$ -position D1 and D2 (**6a** and **6b**) and the two-headed boranophosphate cap analog (**4**) on RNA stability and protein translation in antigen-presenting cells. We prepared *in vitro* transcribed mRNAs encoding the reporter protein luciferase and electroporated them into hiDCs. The effects on protein expression from respective 5'-capped mRNAs were analyzed and compared to the reference caps ( $m^7GpppG$  and  $m_2^{7,3'-O}GpppG$ ) and to the analogously substituted phosphorothioate caps ( $m_2^{7,2'-O}GppspG$  D1 and D2; Figure 1). The latter, especially the D1 diastereomer, was previously shown to substantially increase the amount and duration of protein expression in hiDCs (12).

The effects of differentially 5'-capped mRNAs on protein translation in hiDCs were analyzed by measuring luciferase activity 72 h post-electroporation (Figure 8). Additionally, values for translational efficiency, the time point of maximal protein expression indicative for RNA stability and total protein expression were calculated and are summarized in Table 8. Luciferase kinetics in hiDCs from RNAs into which the cap analogs  $m^7GpppG$ ,  $m_2^{7,3'-O}GpppG$  and  $m_2^{7,2'-O}GppspG$  D1 or  $m_2^{7,2'-O}GppspG$  D2 were inserted were similar to previously published data (12). The  $\beta$ -substitution of a non-bridging oxygen of the triphosphate chain with sulfur results in a significant increase of translational efficiency, functional RNA stability and of the amount of reporter protein produced from the respective RNAs. Although the D2 diastereomer has a stronger effect on initial translational efficiency, incorporation of the D1 diastereomer results in higher stability of the respective mRNA and eventually in a larger quantity of reporter gene product. Effects analogous to those reported for  $\beta$ -S-ARCA (D1 and D2) were observed for the two respective  $BH_3$ -substituted diastereomers D1 and D2 (**6a** and **6b**) on protein expression profiles in hiDCs. Interestingly, not only the ratios of protein expression of D1-to-D2 diastereomers are comparable, but also the absolute increase induced with respect to reference RNAs with unmodified phosphate chains. The total protein expression for the D1

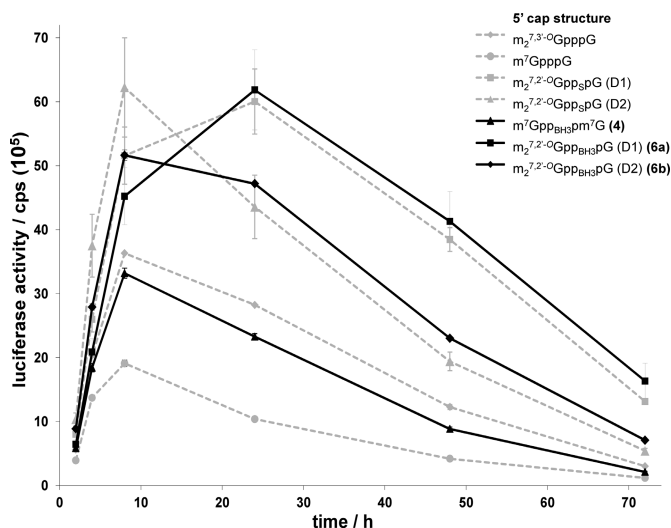


**Figure 8.** The influence of different mRNA cap analogs on luciferase expression in human immature dendritic cells (hiDCs). After electroporation of respective 5'-capped mRNAs into hiDCs, luciferase activity was measured after 2, 4, 8, 24, 48 and 72 h (each experiment was performed in duplicate). The corresponding averaged bioluminescence signals are depicted as a function of time. The data are shown as mean  $\pm$  SD.

diastereomers relative to expression from ARCA-capped RNA was  $2.19 \pm 0.22$  for the phosphorothioate-capped mRNA and  $2.25 \pm 0.35$  for the mRNA carrying the boranophosphate cap **6a**, while the D2 diastereomers result in an increase of  $1.60 \pm 0.25$  and  $1.66 \pm 0.02$ , respectively (Table 8). The third boranophosphate cap tested, the two-headed cap analog with a substitution at the  $\beta$ -position (**4**), yielded an expression profile similar to that observed for unmodified ARCA. Thus, the two headed cap **4**, despite its advantages such as a straightforward synthetic route and pseudo-symmetric structure, is not preferable for augmenting the mRNA expression in hiDCs.

## DISCUSSION

Synthetic cap analogs are recognized by numerous proteins involved in mRNA metabolism and therefore are often used for studying cap-related processes. Increasing knowledge about these processes and a better understanding of pathological changes caused by their deregulation may contribute to the development of cap-based therapeutics. One potential application of small-molecular-weight cap analogs is their use as translation inhibitors in anti-cancer therapy intended to counteract elevated levels of the cap binding translation initiation factor 4E (eIF4E) (14,47). Many types of cancer overexpress this oncogene, and targeting eIF4E through various experimental therapies has been shown to inhibit tumor growth (50). Several cap-derived translation inhibitors targeting eIF4E have also been proposed and some of them appear to be effective in cell lysates or in cultured cells (22,51–54). However, several problems associated with therapeutic applications of cap analogs remain to be solved, including those associated with cap analog stability *in vivo*. All synthetic cap analogs are potential substrates for decapping scavenger enzyme (DcpS). In the cells, DcpS prevents accumu-

lation of small capped (oligo)nucleotides (released as a result of mRNA turnover in the 3' → 5' route) that could interfere with cap-related processes (17,18). Hence, DcpS would also pose a threat for intracellular delivered cap-derived (di)nucleoside oligophosphates designed for therapeutic applications. Therefore, developing and studying DcpS-resistant cap analogs may not only provide new insights into the mechanisms of decapping but also benefit the development of new inhibitors of cap-recognizing proteins. Moreover, DcpS itself has been identified as a therapeutic target in spinal muscular atrophy (55).

Synthetic cap analogs are also utilized for the synthesis of 5'-capped mRNAs by co-transcriptional capping. Using this method along with appropriately designed cap analogs, one can site-specifically introduce various chemical modifications into the 5' end of mRNA. The modifications may affect intrinsic properties of mRNA such as stability and translational efficiency, and this has been recently exploited for tuning properties of transcripts dedicated for therapeutic applications of exogenously delivered mRNAs.

Our main goal in this work was to synthesize and characterize a novel class of cap analogs—boranophosphate analogs (or BH<sub>3</sub>-analogs) and verify their utility as a tool for manipulation of the above-mentioned cap-dependent processes. We achieved this by developing efficient synthetic methods for BH<sub>3</sub>-analogs, stereochemical and physicochemical characterization of the synthesized compounds and finally studying their biochemical properties *in vitro* and *in vivo*.

### Synthesis and physicochemical properties of BH<sub>3</sub>-analogs

The synthesis of boranophosphate analogs of nucleoside oligophosphates is usually accomplished by taking advantage of the reactivity of trivalent phosphorus derivatives. Several approaches for the synthesis of boranophosphate-containing mono- and dinucleoside oligophosphates have been developed on the basis of trivalent phosphorus chemistry, most of which encompass a reaction sequence consisting of 5'-phosphitylation of a suitably protected nucleoside, new pyrophosphate bond formation via a reaction with a phosphate-nucleophile, boronation with a BH<sub>3</sub>–Lewis base complex and finally an alkali-mediated removal of the protecting groups (23,41,56–60). However, such approach would not be applicable for our purpose, i.e. to the synthesis of dinucleotide mRNA cap analogs selectively modified with boranophosphate moiety at either α, β or γ-position of the 5',5'-triphosphate bridge. The presence of two not identical nucleoside moieties, one of them being an alkali-sensitive nucleobase, 7-methylguanine, implied the necessity for a multistep, iterative synthesis. Therefore, the synthesis of BH<sub>3</sub>-analogs was carried out by another approach, which involved divalent metal ion-mediated formation of a pyrophosphate bond between phosphate (V) nucleophilic and electrophilic species (39,57,61–62). The optimization studies (Supplementary Table S1) indicate that the main factor influencing efficiency of the formation of a pyrophosphate bond between a nucleoside boranomonomophosphate and a nucleotide imidazolide derivative is the stability of the former. Only if the processes of P-B-bond cleavage in the acidic conditions and hydrolysis of the 5'-phosphoester

bond are suppressed, (63) may a dinucleotide be synthesized efficiently. The efficiencies and complexities of the synthetic paths varied depending on the position of the boranophosphate moiety and presence of additional methylations. However, for all BH<sub>3</sub>-analogs we eventually developed reasonably efficient synthetic pathways that enabled isolation of the target compounds in multi-milligram quantities and should be easily scalable even to multi-grams. In order to make our synthetic approach more general, we tested whether the boranophosphate nucleophiles may be used for the synthesis of other biologically important nucleotides. Consequently, we demonstrated that the approach is applicable not only to mRNA cap analogs but also to α-modified nucleoside triphosphates or double-modified (at the α- and γ-position) dinucleoside triphosphates.

The influence of a boranophosphate group on cap analog conformation was analyzed based on the fluorescence and NMR data. Important determinants of the conformation of dinucleoside oligophosphates in solution are stacking interactions between two nucleoside moieties. As shown in Table 3, the O to BH<sub>3</sub> substitutions generally only slightly affected the extent of stacking. Only for cap analogs for which the γ or α non-bridging *pro-S<sub>P</sub>* oxygen atom was substituted with BH<sub>3</sub> the fraction of stacked conformation was noticeably lower compared to m<sup>7</sup>GpppG, suggesting that these substitutions may somehow affect the overall conformation of the dinucleotide. The data for BH<sub>3</sub>-analogs and their phosphorothioate congeners, S-analogs, corresponded well, indicating for similarities rather than differences between the two modifications. The sugar puckering in BH<sub>3</sub>-analogs determined from <sup>1</sup>H NMR data was also typical. For dinucleotides such as m<sup>7</sup>GpppG, the populations of guanosine *N* (C3'-endo) and *S* (C2'-endo) conformers in dynamic equilibrium are close to the populations of 5'-GMP (65 ± 5% *S* and 35 ± 5% *N*) (27). In contrast, for 7-methylguanosine a characteristic increase in the amount of the *N* conformer occurs (up to 65%), which can be most easily observed in the <sup>1</sup>H NMR spectrum judging by the decrease in the <sup>3</sup>J<sub>H1'-H2'</sub> coupling constant from ~6 Hz to ~3 Hz. For all BH<sub>3</sub>-analogs (1–6) and other nucleotides such as NDPαBH<sub>3</sub> (12, 13, 20), NTPαBH<sub>3</sub> (23, 24), Gpp<sub>BH3</sub>pG (15) and Ap<sub>BH3</sub>pp<sub>BH3</sub>A (21), <sup>1</sup>H-<sup>1</sup>H coupling constant values are close to those for the unmodified parent compounds (Supplementary Table S2). The ribose conformations did not vary between the P-diastereomers. Hence, one can assume that the differences in biological properties between phosphate unmodified analogs, BH<sub>3</sub>-analogs and S-analogs are caused by different geometry and electronic structure of the boranophosphate group rather than by significant conformational changes induced by its presence.

### Recognition by DcpS and eIF4E

The effect of a boranophosphate group on the cap recognition by DcpS and eIF4E was then investigated. As generally expected on the basis of the proposed hDcpS mechanism and studies on previously synthesized cap analogs, the O to BH<sub>3</sub> substitution at the γ-position decreased the susceptibility to DcpS significantly. However, quite surprisingly also BH<sub>3</sub>-analogs modified at the β-position of the triphosphate bridge were resistant to hDcpS, which was in con-

trast to the corresponding  $\beta$ -S-analogs. To find a plausible explanation for the observed differences between  $\beta$ -S- and  $\beta$ -BH<sub>3</sub>-analogs, we analyzed available crystallographic data for hDcpS H277N mutant in complexes with cap analogs, m<sup>7</sup>GpppG (PDB entry 1ST0; (17)) and m<sup>7</sup>GpppA (PDB entry 1ST4) (17) (Figure 9). The structures reveal that hDcpS is a homodimeric protein, which includes two dimeric domains, N- and C-terminal. The DcpS dimer is asymmetric, i.e. if one active site is in the open conformation, then the other is closed. In the crystal structures two cap ligands are coordinated to DcpS, one accommodated in the open and one in the closed conformation on opposite sides of the dimer. Both m<sup>7</sup>GpppG and m<sup>7</sup>GpppA bound at the open site adopt extended conformations with most of the contacts to the protein made by the m<sup>7</sup>G (to Trp 175, Leu 206, Tyr 273 and others) and the  $\gamma$ -phosphate (to His 279 and Tyr 273), and few (if any) by the  $\beta$ - and  $\alpha$ -phosphates or the second nucleoside (G or A) (Figure 9). In the closed conformation, the m<sup>7</sup>G and  $\gamma$ -phosphate make virtually the same contacts as in the open conformation, but additional contacts are made by the  $\beta$ - and  $\alpha$ -phosphates and the second nucleoside. The closed cap-binding pocket is much tighter, which results in a characteristic ‘bent’ alignment of the triphosphate bridge (Figure 9). The  $\beta$ -phosphate, which serves as a leaving group in the catalytic process, is stabilized in the closed state by numerous hydrogen bonds to side chains of Ser 272, Lys 142 and Arg 294, although functional studies revealed that those amino acids are not essential for catalytic activity as much as e.g. His 277 or His 279 (18). The somehow different alignment of the  $\alpha$ - and  $\beta$ -phosphates for m<sup>7</sup>GpppG and m<sup>7</sup>GpppA suggests that some structural flexibility of the triphosphate bridge is still possible even in the closed conformation (17). The resistance of  $\gamma$ -BH<sub>3</sub> and  $\gamma$ -S-analogs may result from disruption of the transition state geometry by the S or BH<sub>3</sub> substituents, because they are more bulky than oxygen. In the case of the  $\beta$ -borano cap analogs, the resistance to hDcpS could also result from the bulkiness of the BH<sub>3</sub> group compared to oxygen. However, we consider this hypothesis less likely to be true, because the corresponding S-analogs are readily hydrolyzed by DcpS and there is very little structural difference between boranophosphates and phosphorothioates in terms of bond lengths, geometry and bulkiness as well as the spectroscopic characterization indicated very little influence of the  $\beta$ -phosphate modifications on the overall conformation of a cap analog. Alternatively, due to the lack of H-bond acceptor properties of the BH<sub>3</sub> group, the  $\beta$ -phosphate may not be sufficiently stabilized by the surrounding amino acid side chains to serve as a good leaving group (17). The relatively low binding affinity of all BH<sub>3</sub>-analogs compared to other hDcpS-resistant analogs (Table 6) indirectly supports such assumption. Interestingly, *Ce*DcpS recognizes BH<sub>3</sub>-analogs with different specificity. In particular, the  $\beta$ -BH<sub>3</sub>-analogs are more readily hydrolyzed than by hDcpS. Only  $\gamma$ -modified analog **3a** was sufficiently stable under high *Ce*DcpS concentrations in order to determine the  $K_{AS}$  value for the complex, whereas for hDcpS  $K_{AS}$  values was determined for six analogs (**2a**, **2b**, **3a**, **4**, **6a** and **6b**). These observations are in general agreement with the current knowledge on *Ce*DcpS, which has a broader substrate specificity than hDcpS (45). Nonetheless, both enzymes share com-

mon stereoselectivity by hydrolyzing the *R<sub>P</sub>* isomer of  $\gamma$ -BH<sub>3</sub>-analog of configuration (**3b**), but not the *S<sub>P</sub>* isomer (**3a**). Unfortunately, neither apo nor cap-bound X-ray structures have been reported yet for *Ce*DcpS. The comparison of structures of the two enzymes in the context of observed similarities and differences in susceptibility of BH<sub>3</sub>-analogs could provide an interesting mechanistic insight into the DcpS enzymes in the future. It is worth mentioning that in a related biological study (35), compounds **4**, **6a** and **6b** were shown to render mRNA resistant to the decapping enzyme Dcp2, which, in contrast to DcpS, uses long capped RNAs as a substrate and cleaves the cap between  $\alpha$ - and  $\beta$ -phosphates. Accordingly, this single  $\beta$ -BH<sub>3</sub> for O substitution is the first described cap modification that makes the cap resistant to both decapping enzymes, DcpS and Dcp2, differing in their substrate-selectivity and regioselectivity.

The binding affinities for hDcpS, *Ce*DcpS and eIF4E provide further information on how the boranophosphate group influences interactions of cap analogs with proteins. Interestingly, the O to BH<sub>3</sub> substitution has opposite effects on the binding to DcpS and to eIF4E. For eIF4E, the effect of O to BH<sub>3</sub> substitution is generally stabilizing. The affinity of BH<sub>3</sub> analogs for eIF4E varied depending on the position and stereochemistry of the substitution, but was either equal to or higher than affinity of m<sup>7</sup>GpppG reference complex (Table 5), making the cap BH<sub>3</sub>-analogs (next to the S-analogs) the strongest phosphate-modified binders of eIF4E. In contrast, the affinities for hDcpS were generally lower compared with other cap analogs, making the cap BH<sub>3</sub>-analogs one of the poorest phosphate-modified ligands for DcpS (Table 6). These striking differences may be explained on the basis of the properties of the two cap-binding pockets. The eIF4E's binding site is rather loose with a hydrophilic, positively charged slot responsible for electrostatic interactions with the negatively charged triphosphate chain of the cap. Since these interactions are crucial for the stabilization of the cap-eIF4E, high  $K_{AS}$  values for BH<sub>3</sub>-analogs indicate that the boranophosphate group is capable of maintaining electrostatic interactions with proteins, similarly as S-analogs. In contrast, the cap-binding site of hDcpS in the closed conformation is rather tight and provides numerous close H-bond contacts to the ligand bound. Accordingly, it has been found that various cap modifications that are generally accepted by eIF4E may significantly diminish affinity to hDcpS. The binding affinities of BH<sub>3</sub>-analogs to hDcpS were low compared to all other types of phosphate-modified cap analogs, including roughly 2-fold lower than affinities of corresponding S-analogs. These differences might be a consequence of the inability of the BH<sub>3</sub>-group to accept H-bonds, in contrast to S or O atoms. The DcpS-related differences between BH<sub>3</sub>- and S-analogs illustrate how boranophosphate and phosphorothioate nucleotides, though generally considered close mimics, can differ significantly in their biological activity.

### BH<sub>3</sub>-analogs as inhibitors of translation

Some of the BH<sub>3</sub>-analogs with higher affinity for the eIF4E translation factor and lower affinity and susceptibility to hDcpS than the native cap might serve as potent and selec-



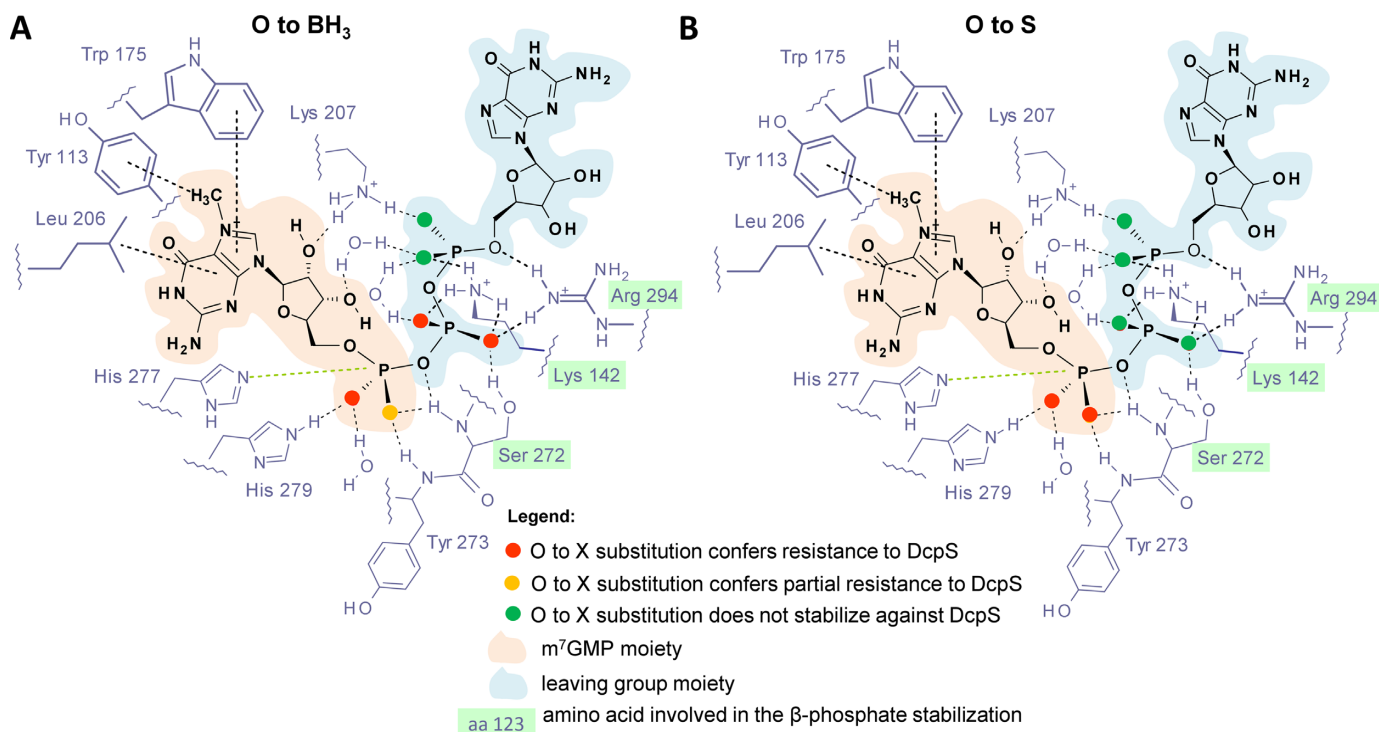


**Figure 9.** Effects of non-bridging phosphate chain modifications on the susceptibility of cap dinucleotides to cleavage by human DcpS: comparison between BH<sub>3</sub>-analogs (A) and S-analogs (B). The schematic map of plausible protein–ligand interactions is based on crystallographic structure of a catalytically inactivated hDcpS mutant (His 277→Asp) in complex with m<sup>7</sup>GpppG (PDB entry 1ST0 (17)). The main difference between the O to BH<sub>3</sub> and O to S substitutions is that the β-BH<sub>3</sub> substitutions produce DcpS-resistant analogs, whereas corresponding β-S-analogs are good substrates for DcpS. A possible explanation is that the β-boranophosphate moiety, due to insufficient ability of the BH<sub>3</sub> substituent to form hydrogen bonds, cannot be sufficiently stabilized as a leaving group by the basic amino acid residues in DcpS's cap-binding pocket. Some ribose and nucleobase interactions have been omitted for clarity.

tive inhibitors of protein translation that could counteract elevated levels of eIF4E in cancer cells. The inhibitory potency of the compounds was hence tested *in vitro* in RRLs. Two experimental setups A and B were used, one for testing the inhibitory potency alone and the other for testing the inhibitory potency in combination with functional cap stability in RRL (Table 7). All BH<sub>3</sub>-analogs were potent inhibitors in the first setup, but in the second setup only analogs that were identified as DcpS-resistant remained potent. This result agrees with our previous findings for other DcpS-resistant compounds and points to a positive correlation between susceptibility of an analog to DcpS and inhibitory properties (22). It also indicates that if the affinity for eIF4E is sufficiently high, other factors, such as stability, determine the performance of a given cap analog as a translation inhibitor. The increased stability in RRL for DcpS-resistant compounds indicates that degradation of cap analogs in RRL occurs mainly by the pyrophosphate-bond cleavage between γ- and β-phosphates, which may be carried out by a DcpS-like activity present in RRL (such cleavage would produce m<sup>7</sup>GMP-type compound, a relatively poor eIF4E binder and thus poor inhibitor of translation). Due to combination of a relatively straightforward synthetic route, high affinity to eIF4E, low affinity to DcpS, strong inhibitory activity and high stability, compound **2a** appears as a most promising candidate for future *in vivo* studies in combination with novel nucleotide-delivery strategies (64–67).

### Translation of mRNAs capped with BH<sub>3</sub>-analogs in dendritic cells

The β-BH<sub>3</sub>-analogs **4**, **6a** and **6b** were also incorporated into mRNA transcripts and shown to influence stability and expression of mRNA in dendritic cells (Table 8 and Figure 8). One important parameter in the context of anti-cancer vaccination is the total protein expression indicating mRNA translational efficiency and functional stability. mRNA capped with analog **6a** performed most efficiently and, hence, was identified as the best candidate for this purpose. A plausible explanation for the favorable properties of this analog might be the ~2-fold higher *K*<sub>AS</sub> of the D1 diastereomers to eIF4E (7,35). In contrast, in other tested eukaryotic expression systems (HeLa cells and RRL) the D2-capped RNAs, which are more resistant against degradation by the decapping enzyme, are more efficiently translated than their D1 counterparts (35), indicating cell-type-specific dependencies. The ARCA BH<sub>3</sub>-analogs (**6a** and **6b**) performed at least as well as the corresponding S-analogs, which indicates that both modifications are equally acceptable in terms of requirements of the translational system.

While the results of our studies, taken altogether, revealed that there is no simple correlation between the effects of the cap analog modification and either stability or properties as translation promoters (when introduced into mRNA) or translation inhibitors (when used as free molecules), we can conclude that the best candidates for manipulating mRNA translation are analogs modified at the β-position of the

triphosphate bridge: compound **2a** and its ARCA equivalent **6a**. These compounds are characterized by high affinity for eIF4E, poor affinity for hDcpS and either lowest IC<sub>50</sub> as inhibitor of translation (compound **2a**) or best translation properties (highest total protein expression) *in vivo* when introduced into mRNA (compound **2a**; Tables 5–8). The results indicate also that the phosphorothioate and boranophosphate groups, despite their close structural and functional similarities, can also differ in their phosphate mimicking features, which indicates that one should not assume in advance that the nucleotides from the two families will have identical biological features and provides a rationale for independent testing in new biological systems.

## SUPPLEMENTARY DATA

Supplementary Data are available at NAR Online.

## ACKNOWLEDGMENTS

The authors are grateful to the Laboratory of Biological NMR (Institute of Biochemistry and Biophysics of the Polish Academy of Sciences, IBB PAS, Warsaw) for access to their NMR apparatus, and to Jacek Oledzki from the Laboratory of Mass Spectrometry (IBB PAS) for recording HRMS spectra.

## FUNDING

National Science Centre, Poland [2011/01/D/ST5/05869 to J.K.; 2012/05/E/ST5/03893 to J.J.; UMO-2011/01/N/NZ1/04326 to M.Z.; 2013/08/A/NZ1/00866, 2012/07/B/NZ1/00118 to E.D.]; National Centre of Development and Research, Poland [02/EuroNanoMed/2011 to E.D.]; Innotech Program of the State of Rhineland-Palatinate, Germany [to U.S.]; National Institutes of Health, USA [R01GM20818 to R.E.R.]; Foundation for Polish Science International Ph.D. Projects Programme, EU European Regional Development Fund [to M.Z. and M.S.]. Funding for open access charge: National Science Centre (Poland).

*Conflict of interest statement.* None declared.

## REFERENCES

- Coller, J. and Parker, R. (2004) Eukaryotic mRNA decapping. *Annu. Rev. Biochem.*, **73**, 861–890.
- Sonenberg, N. (2008) eIF4E, the mRNA cap-binding protein: from basic discovery to translational research. *Biochem. Cell Biol.*, **86**, 178–183.
- Cougot, N., van Dijk, E., Babajko, S. and Séraphin, B. (2004) 'Cap-tabolism'. *Trends Biochem. Sci.*, **29**, 436–444.
- Gonatopoulos-Pournatzis, T. and Cowling, V.H. (2014) Cap-binding complex (CBC). *Biochem. J.*, **457**, 231–242.
- Rhoads, R.E. (2009) eIF4E: new family members, new binding partners, new roles. *J. Biol. Chem.*, **284**, 16711–16715.
- Kalek, M., Jemielity, J., Darzynkiewicz, Z.M., Bojarska, E., Stepinski, J., Stolarski, R., Davis, R.E. and Darzynkiewicz, E. (2006) Enzymatically stable 5' mRNA cap analogs: synthesis and binding studies with human DcpS decapping enzyme. *Bioorg. Med. Chem.*, **14**, 3223–3230.
- Kowalska, J., Lewdorowicz, M., Zuberek, J., Grudzien-Nogalska, E., Bojarska, E., Stepinski, J., Rhoads, R.E., Darzynkiewicz, E., Davis, R.E. and Jemielity, J. (2008) Synthesis and characterization of mRNA cap analogs containing phosphorothioate substitutions that bind tightly to eIF4E and are resistant to the decapping pyrophosphatase DcpS. *RNA*, **14**, 1119–1131.
- Rydzik, A.M., Lukaszewicz, M., Zuberek, J., Kowalska, J., Darzynkiewicz, Z.M., Darzynkiewicz, E. and Jemielity, J. (2009) Synthetic dinucleotide mRNA cap analogs with tetraphosphate 5',5' bridge containing methylenebis(phosphonate) modification. *Org. Biomol. Chem.*, **7**, 4763–4776.
- Rydzik, A.M., Kulis, M., Lukaszewicz, M., Kowalska, J., Zuberek, J., Darzynkiewicz, Z.M., Darzynkiewicz, E. and Jemielity, J. (2012) Synthesis and properties of mRNA cap analogs containing imidodiphosphate moiety—fairly mimicking natural cap structure, yet resistant to enzymatic hydrolysis. *Bioorg. Med. Chem.*, **20**, 1699–1710.
- Grudzien-Nogalska, E., Jemielity, J., Kowalska, J., Darzynkiewicz, E. and Rhoads, R.E. (2007) Phosphorothioate cap analogs stabilize mRNA and increase translational efficiency in mammalian cells. *RNA*, **13**, 1745–1755.
- Grudzien, E., Kalek, M., Jemielity, J., Darzynkiewicz, E. and Rhoads, R.E. (2006) Differential inhibition of mRNA degradation pathways by novel cap analogs. *J. Biol. Chem.*, **281**, 1857–1867.
- Kuhn, A.N., Diken, M., Kreiter, S., Selmi, A., Kowalska, J., Jemielity, J., Darzynkiewicz, E., Huber, C., Tureci, O. and Sahin, U. (2010) Phosphorothioate cap analogs increase stability and translational efficiency of RNA vaccines in immature dendritic cells and induce superior immune responses *in vivo*. *Gene Ther.*, **17**, 961–971.
- Zdanowicz, A., Thermann, R., Kowalska, J., Jemielity, J., Duncan, K., Preiss, T., Darzynkiewicz, E. and Hentze, M.W. (2009) Drosophila miR2 primarily targets the m(7)GpppN cap structure for translational repression. *Mol. Cell*, **35**, 881–888.
- Jemielity, J., Kowalska, J., Rydzik, A.M. and Darzynkiewicz, E. (2010) Synthetic mRNA cap analogs with a modified triphosphate bridge—synthesis, applications and prospects. *New J. Chem.*, **34**, 829–844.
- Stepinski, J., Waddell, C., Stolarski, R., Darzynkiewicz, E. and Rhoads, R.E. (2001) Synthesis and properties of mRNAs containing the novel "anti-reverse" cap analogs 7-methyl(3'-O-methyl)GpppG and 7-methyl(3'-deoxy)GpppG. *RNA*, **7**, 1486–1495.
- Grudzien-Nogalska, E., Stepinski, J., Jemielity, J., Zuberek, J., Stolarski, R., Rhoads, R.E. and Darzynkiewicz, E. (2007) Synthesis of anti-reverse cap analogs (ARCAs) and their applications in mRNA translation and stability. *Methods Enzymol.*, **431**, 203–227.
- Gu, M.G., Fabrega, C., Liu, S.W., Liu, H.D., Kiledjian, M. and Lima, C.D. (2004) Insights into the structure, mechanism, and regulation of scavenger mRNA decapping activity. *Mol. Cell*, **14**, 67–80.
- Liu, S.W., Jiao, X.F., Liu, H.D., Gu, M.G., Lima, C.D. and Kiledjian, M. (2004) Functional analysis of mRNA scavenger decapping enzymes. *RNA*, **10**, 1412–1422.
- Hsieh, A.C. and Ruggero, D. (2010) Targeting eukaryotic translation initiation factor 4E (eIF4E) in cancer. *Clin. Cancer Res.*, **16**, 4914–4920.
- Fischer, P.M. (2009) Cap in hand: targeting eIF4E. *Cell Cycle*, **8**, 2535–2541.
- Graff, J.R., Konicek, B.W., Carter, J.H. and Marcusson, E.G. (2008) Targeting the eukaryotic translation initiation factor 4E for cancer therapy. *Cancer Res.*, **68**, 631–634.
- Kowalska, J., Lukaszewicz, M., Zuberek, J., Ziemniak, M., Darzynkiewicz, E. and Jemielity, J. (2009) Phosphorothioate analogs of m(7)GTP are enzymatically stable inhibitors of cap-dependent translation. *Bioorg. Med. Chem. Lett.*, **19**, 1921–1925.
- Li, P., Sergueeva, Z.A., Dobrikov, M. and Shaw, B.R. (2007) Nucleoside and oligonucleoside boranophosphates: chemistry and properties. *Chem. Rev.*, **107**, 4746–4796.
- Cheek, M.A., Sharaf, M.L., Dobrikov, M.I. and Shaw, B.R. (2013) Inhibition of hepatitis C viral RNA-dependent RNA polymerase by  $\alpha$ -P-boranophosphate nucleotides: exploring a potential strategy for mechanism-based HCV drug design. *Antivir. Res.*, **98**, 144–152.
- Shaw, B.R., Dobrikov, M., Wang, X., Wan, J., He, K.Z., Lin, J.L., Li, P., Rait, V., Sergueeva, Z.A. and Sergueev, D. (2003) Reading, writing, and modulating genetic information with boranophosphate mimics of nucleotides, DNA, and RNA. *Ann. N.Y. Acad. Sci.*, **1002**, 12–29.
- Roy, S., Olesiak, M., Padar, P., McCuen, H. and Caruthers, M.H. (2012) Reduction of metal ions by boranophosphonate DNA. *Org. Biomol. Chem.*, **10**, 9130–9133.

27. Jemielity, J., Fowler, T., Zuberek, J., Stepinski, J., Lewdorowicz, M., Niedzwiecka, A., Stolarski, R., Darzynkiewicz, E. and Rhoads, R.E. (2003) Novel "anti-reverse" cap analogs with superior translational properties. *RNA*, **9**, 1108–1122.
28. Cai, A., Jankowska-Anyszka, M., Centers, A., Chlebicka, L., Stepinski, J., Stolarski, R., Darzynkiewicz, E. and Rhoads, R.E. (1999) Quantitative assessment of mRNA cap analogs as inhibitors of in vitro translation. *Biochemistry*, **38**, 8538–8547.
29. Grudzien, E., Stepinski, J., Jankowska-Anyszka, M., Stolarski, R., Darzynkiewicz, E. and Rhoads, R.E. (2004) Novel cap analogs for in vitro synthesis of mRNAs with high translational efficiency. *RNA*, **10**, 1479–1487.
30. Wieczorek, Z., Zdanowski, K., Chlebicka, L., Stepinski, J., Jankowska, M., Kierdaszuk, B., Temeriusz, A., Darzynkiewicz, E. and Stolarski, R. (1997) Fluorescence and NMR studies of intramolecular stacking of mRNA cap-analogs. *Biochim. Biophys. Acta*, **1354**, 145–152.
31. Wypijewska del Noga, A., Surleac, M.D., Kowalska, J., Lukaszewicz, M., Jemielity, J., Bisaillon, M., Darzynkiewicz, E., Milac, A.L. and Bojarska, E. (2013) Analysis of decapping scavenger cap complex using modified cap analogs reveals molecular determinants for efficient cap binding. *FEBS J.*, **280**, 6508–6527.
32. Niedzwiecka, A., Stepinski, J., Antosiewicz, J.M., Darzynkiewicz, E. and Stolarski, R. (2007) Translation Initiation: Cell Biology, High-throughput Methods, and Chemical-based Approaches. In: Jon, L. (ed). *Method Enzymol.*, **430**, Elsevier Academic Press Inc., San Diego, CA, pp. 209–245.
33. DeAngelis, M.M., Wang, D.G. and Hawkins, T.L. (1995) Solid-phase reversible immobilization for the isolation of PCR products. *Nucleic Acids Res.*, **23**, 4742–4743.
34. Zuberek, J., Jemielity, J., Jablonowska, A., Stepinski, J., Dadlez, M., Stolarski, R. and Darzynkiewicz, E. (2004) Influence of electric charge variation at residues 209 and 159 on the interaction of eIF4E with the mRNA 5' terminus. *Biochemistry*, **43**, 5370–5379.
35. Su, W., Slepencov, S., Grudzien-Nogalska, E., Kowalska, J., Kulis, M., Zuberek, J., Lukaszewicz, M., Darzynkiewicz, E., Jemielity, J. and Rhoads, R.E. (2011) Translation, stability, and resistance to decapping of mRNAs containing caps substituted in the triphosphate chain with BH3, Se, and NH. *RNA*, **17**, 978–988.
36. Darzynkiewicz, Z.M., Bojarska, E., Kowalska, J., Lewdorowicz, M., Jemielity, J., Kalek, M., Stepinski, J., Davis, R.E. and Darzynkiewicz, E. (2007) Interaction of human decapping scavenger with 5' mRNA cap analogs: structural requirements for catalytic activity. *J. Phys.-Condens. Mat.*, **19**, 285217.
37. Wypijewska, A., Bojarska, E., Lukaszewicz, M., Stepinski, J., Jemielity, J., Davis, R.E. and Darzynkiewicz, E. (2012) 7-methylguanosine diphosphate (m7GDP) Is not hydrolyzed but strongly bound by decapping scavenger (DcpS) enzymes and potently inhibits their activity. *Biochemistry*, **51**, 8003–8013.
38. Strenkowska, M., Kowalska, J., Lukaszewicz, M., Zuberek, J., Su, W., Rhoads, R.E., Darzynkiewicz, E. and Jemielity, J. (2010) Towards mRNA with superior translational activity: synthesis and properties of ARCA tetraphosphates with single phosphorothioate modifications. *New J. Chem.*, **34**, 993–1007.
39. Strenkowska, M., Wanat, P., Ziemniak, M., Jemielity, J. and Kowalska, J. (2012) Preparation of synthetically challenging nucleotides using cyanoethyl P-imidazolides and microwaves. *Org. Lett.*, **14**, 4782–4785.
40. Yanachkov, I.B., Dix, E.J., Yanachkova, M.I. and Wright, G.E. (2011) P1, P2-Diimidazolyl derivatives of pyrophosphate and bis-phosphonates—synthesis, properties, and use in preparation of dinucleoside tetraphosphates and analogs. *Org. Biomol. Chem.*, **9**, 730–738.
41. Li, P., Xu, Z.H., Liu, H.Y., Wennefors, C.K., Dobrikov, M.I., Ludwig, J. and Shaw, B.R. (2005) Synthesis of alpha-P-modified nucleoside Diphosphates with ethylenediamine. *J. Am. Chem. Soc.*, **127**, 16782–16783.
42. Major, D.T., Nahum, V., Wang, Y.F., Reiser, G. and Fischer, B. (2004) Molecular recognition in purinergic receptors. 2. Diastereoselectivity of the h-P2Y(1)-receptor. *J. Med. Chem.*, **47**, 4405–4416.
43. Liu, H., Rodgers, N.D., Jiao, X. and Kiledjian, M. (2002) The scavenger mRNA decapping enzyme DcpS is a member of the HIT family of pyrophosphatases. *EMBO J.*, **21**, 4699–4708.
44. Cohen, L.S., Mikhli, C., Friedman, C., Jankowska-Anyszka, M., Stepinski, J., Darzynkiewicz, E. and Davis, R.E. (2004) Nematode m7GpppG and m32,2,7GpppG decapping: activities in *Ascaris* embryos and characterization of *C. elegans* scavenger DcpS. *RNA*, **10**, 1609–1624.
45. Wypijewska, A., Bojarska, E., Stepinski, J., Jankowska-Anyszka, M., Jemielity, J., Davis, R.E. and Darzynkiewicz, E. (2010) Structural requirements for *Caenorhabditis elegans* DcpS substrates based on fluorescence and HPLC enzyme kinetic studies. *FEBS J.*, **277**, 3003–3013.
46. Niedzwiecka, A., Marcotrigiano, J., Stepinski, J., Jankowska-Anyszka, M., Wyslouch-Cieszynska, A., Dadlez, M., Gingras, A.C., Mak, P., Darzynkiewicz, E., Sonenberg, N. et al. (2002) Biophysical studies of eIF4E cap-binding protein: recognition of mRNA 5' cap structure and synthetic fragments of eIF4G and 4E-BP1 proteins. *J. Mol. Biol.*, **319**, 615–635.
47. Ziemniak, M., Strenkowska, M., Kowalska, J. and Jemielity, J. (2013) Potential therapeutic applications of RNA cap analogs. *Future Med. Chem.*, **5**, 1141–1172.
48. Su, W., Slepencov, S.V., Slevin, M.K., Lyons, S.M., Ziemniak, M., Kowalska, J., Darzynkiewicz, E., Jemielity, J., Marzluff, W.F. and Rhoads, R.E. (2013) mRNAs containing the histone 3' stem-loop are degraded primarily by decapping mediated by oligouridylation of the 3' end. *RNA*, **19**, 1–16.
49. Kreiter, S., Selmi, A., Diken, M., Koslowski, M., Britten, C.M., Huber, C., Türeci, Ö. and Sahin, U. (2011) Intranodal vaccination with naked antigen-encoding RNA elicits potent prophylactic and therapeutic antitumoral immunity. *Cancer Res.*, **70**, 9031–9040.
50. Graff, J.R., Konicek, B.W., Vincent, T.M., Lynch, R.L., Monteith, D., Weir, S.N., Schwier, P., Capen, A., Goode, R.L., Dowless, M.S. et al. (2007) Therapeutic suppression of translation initiation factor eIF4E expression reduces tumor growth without toxicity. *J. Clin. Invest.*, **117**, 2638–2648.
51. Chen, X., Kopecky, D.J., Mihalic, J., Jeffries, S., Min, X., Heath, J., Deignan, J., Lai, S., Fu, Z., Guimaraes, C. et al. (2012) Structure-guided design, synthesis, and evaluation of guanine-derived inhibitors of the eIF4E mRNA–cap interaction. *J. Med. Chem.*, **55**, 3837–3851.
52. Li, S., Jia, Y., Jacobson, B., McCauley, J., Kratzke, R., Bitterman, P.B. and Wagner, C.R. (2013) Treatment of breast and lung cancer cells with a N-7 benzyl guanosine monophosphate tryptamine phosphoramidate pronucleotide (4Ei-1) results in chemosensitization to gemcitabine and induced eIF4E proteasomal degradation. *Mol. Pharm.*, **10**, 523–531.
53. Ghosh, B., Benyumov, A.O., Ghosh, P., Jia, Y., Avdulov, S., Dahlberg, P.S., Peterson, M., Smith, K., Polunovsky, V.A., Bitterman, P.B. et al. (2009) Nontoxic chemical eradication of the epithelial-to-mesenchymal transition by targeting cap-dependent translation. *ACS Chem. Biol.*, **4**, 367–377.
54. Piecyk, K. and Jankowska-Anyszka, M. (2014) Chemical conjugation of an mRNA cap analog with a cell-penetrating peptide as a potential membrane permeable translation inhibitor. *Tetrahedron Lett.*, **55**, 606–609.
55. Singh, J., Salcius, M., Liu, S.W., Staker, B.L., Mishra, R., Thurmond, J., Michaud, G., Mattoon, D.R., Printen, J., Christensen, J. et al. (2008) DcpS as a therapeutic target for spinal muscular atrophy. *ACS Chem. Biol.*, **3**, 711–722.
56. Han, Q.W., Sarafianos, S.G., Arnold, E., Parniak, M.A., Gaffney, B.L. and Jones, R.A. (2009) Synthesis of boranoate, selenoate, and thioate analogs of AZTp(4)A and Ap(4)A. *Tetrahedron*, **65**, 7915–7920.
57. Yelovitch, S., Camden, J., Weisman, G.A. and Fischer, B. (2012) Boranophosphate isoster controls P2Y-receptor subtype selectivity and metabolic stability of dinucleoside polyphosphate analogs. *J. Med. Chem.*, **55**, 437–448.
58. Haas, M., Ben-Moshe, I., Fischer, B. and Reiser, G. (2013) Sp-2-propylthio-ATP- $\alpha$ -B and Sp-2-propylthio-ATP- $\alpha$ -B,  $\beta$ - $\gamma$ -dichloromethylene are novel potent and specific agonists of the human P2Y11 receptor. *Biochem. Pharmacol.*, **86**, 645–655.
59. Fujita, S., Oka, N., Matsumura, F. and Wada, T. (2011) Synthesis of Oligo( $\alpha$ -d-glycosyl phosphate) derivatives by a phosphoramidite method via boranophosphate intermediates. *J. Org. Chem.*, **76**, 2648–2659.
60. Enya, Y., Nagata, S., Masutomi, Y., Kitagawa, H., Takagaki, K., Oka, N., Wada, T., Ohgi, T. and Yano, J. (2008) Chemical synthesis of diastereomeric diadenosine boranophosphates (ApbA) from

- 2'-O-(2-cyanoethoxymethyl)adenosine by the boranophosphotriester method. *Bioorg. Med. Chem.*, **16**, 9154–9160.
61. Nahum, V., Tulapurkar, M., Levesque, S.A., Sevigny, J., Reiser, G. and Fischer, B. (2006) Diadenosine and diuridine poly(borano)phosphate analogs: synthesis, chemical and enzymatic stability, and activity at P2Y(1) and P2Y(2) receptors. *J. Med. Chem.*, **49**, 1980–1990.
62. Eliahu, S., Lecka, J., Reiser, G., Haas, M., Bigonnesse, F., Levesque, S.A., Pelletier, J., Sevigny, J. and Fischer, B. (2010) Diadenosine 5',5''-(boranated)polyphosphonate analogs as selective nucleotide pyrophosphatase/phosphodiesterase inhibitors. *J. Med. Chem.*, **53**, 8485–8497.
63. Xu, Z., Sergueeva, Z.A. and Shaw, B.R. (2013) Synthesis and hydrolytic properties of thymidine boranomonophosphate. *Tetrahedron Lett.*, **54**, 2882–2885.
64. Caron, J., Reddy, L.H., Lepître-Mouelhi, S., Wack, S., Clayette, P., Rogez-Kreuz, C., Yousfi, R., Couvreur, P. and Desmaële, D. (2010) Squalenoyl nucleoside monophosphate nanoassemblies: new prodrug strategy for the delivery of nucleotide analogs. *Bioorg. Med. Chem. Lett.*, **20**, 2761–2764.
65. Galmarini, C.M., Warren, G., Senanayake, M.T. and Vinogradov, S.V. (2010) Efficient overcoming of drug resistance to anticancer nucleoside analogs by nanodelivery of active phosphorylated drugs. *Int. J. Pharm.*, **395**, 281–289.
66. Giacalone, G., Bochot, A., Fattal, E. and Hillaireau, H. (2013) Drug-induced nanocarrier assembly as a strategy for the cellular delivery of nucleotides and nucleotide analogs. *Biomacromolecules*, **14**, 737–742.
67. Kijewska, K., Jarzębińska, A., Kowalska, J., Jemielity, J., Kepińska, D., Szczytko, J., Pisarek, M., Wiktorska, K., Stolarski, J., Krysiński, P. *et al.* (2013) Magnetic-nanoparticle-decorated polypyrrole microvessels: toward encapsulation of mRNA cap analogs. *Biomacromolecules*, **14**, 1867–1876.